

國立交通大學

電信工程研究所

碩士論文

非理想通道資訊及時空關連通道下之空間調變信號偵測

Detection of SM Signals in the Presence of CSI Error and Spatio-Temporal
Correlation

研究生：張軒誠

指導教授：蘇育德 教授

中華民國一百零二年七月

非理想通道資訊及時空關連通道下之空間調變信號偵測
Detection of Detection of SM Signals in the Presence of CSI Error and
Spatio-Temporal Correlation


研究生：張軒誠

Student : Hsuan-Cheng Chang

指導教授：蘇育德

Advisor : Dr. Yu T. Su

國立交通大學
電信工程研究所
碩士論文



A Thesis
Submitted to the Institute of Communications Engineering
in partial fulfillment of the requirements
for the Degree of
Master of Science
in
Communications Engineering
at the
National Chiao Tung University

July 2013

Hsinchu, Taiwan, Republic of China

公元 2013 年七月

非理想通道資訊及時空關連通道下之空間調變信號偵測

學生：張軒誠

指導教授：蘇育德

國立交通大學

電信工程研究所碩士班

摘 要

空間調變(SM)是一個高效率的多天線傳輸方法。它沒有傳統多天線系統中通道間交互干擾(ICI) 的問題、不需建立多傳輸天線資料鏈的同步，傳送端只需要一個射頻鏈路(RF chain)並可將資訊置於傳送天線序號中。

為偵測、解調 SM 訊號，接收端需有通道資訊(CSI)。大多數的研究都假設通道是非時變的(time-invariant)並有完整正確的 CSI，這樣的假設並不實際。此外一般的 CSI 通道估計演算通常忽略或是不考慮通道的空間與時間的關連性(spatial and temporal correlations)，其推論或估測之正確性有頗多改善的餘地。

本論文探討了決策引導(decision-directed)與基於模型(model-based) 兩種 CSI 估測法。我們同時考慮通道估計誤差(CSI estimation error)及其時空關連性並分別推導相關的最佳解調器。

此外，我們進一步提出了兩種可大幅降低解調器運算複雜度的解調器結構。針對所提出的各種解調器結構，我們透過了電腦模擬來檢驗其效能並與現有的方法比較。這些數據顯示我們所提出的空間調變解調器改善了現有解調器的效能，且低運算複雜度的解調器與最佳解調器的效能差別幾乎是可忽略的。

Detection of SM Signals in the Presence of CSI

Error and Spatio-Temporal Correlation

Student : Hsuan-Cheng Chang Advisor : Yu T. Su

Institute of Communications Engineering
National Chiao Tung University

Abstract

Spatial modulation (SM) is a promising multiple antennas based transmission scheme that induces no inter-(spatial) channel interference (ICI) and does not require timing synchronization amongst multiple spatial data streams. It only needs a single radio frequency (RF) chain and can exploit transmit antenna index for carrying extra information to enhance spectral efficiency.

To detect the SM signals, channel state information (CSI) is need at the receive side. Most SM detection studies assume that the channel is time-invariant and CSI is perfectly known. In reality, CSI is never perfect and varies in time. Moreover, spatial correlations among multiple spatial channels exist but are ignored in channel estimation. In this thesis we release the above assumptions and develop a class of decision-directed and a model-based channel estimator.

Based on the proposed channel estimators we derive optimal detectors that take into account both the CSI error and time-spatial correlation. To simplify the optimal detector, we then proposed two low-complexity suboptimal structures for each optimal detector. Computer simulations are carried out to estimate the corresponding performance and numerical results show that the optimal detectors offer performance gain against conventional SM detector and the suboptimal detectors incur negligible performance loss.

致 謝

得以順利完成碩士論文，首先感謝指導教授 蘇育德博士。讓我對通訊研究有正身的領悟，也和我們分享的許多人生經驗。也感謝口試委員蘇賜麟教授、楊谷章教授、吳文榕教授、呂宗津教授提供許多關於研究上的意見，可以補足這份論文的不足以及缺失。

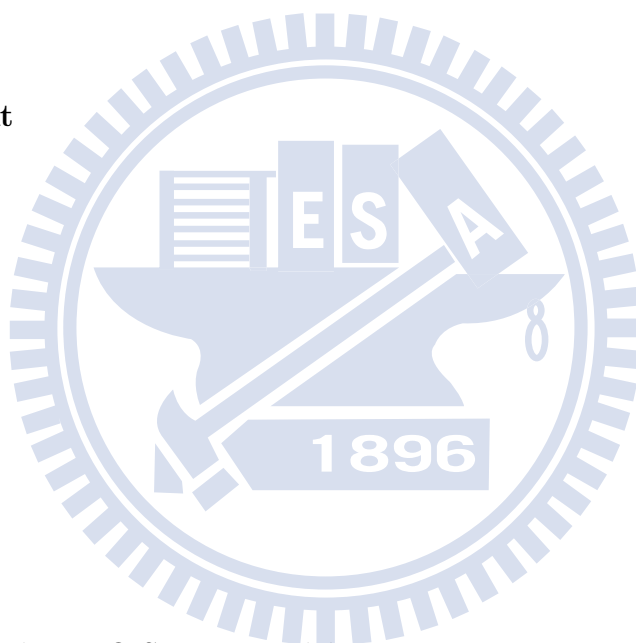
另外，非感謝實驗室的劉彥成學長，給我在做研究上的一些建議以及研究上困難的幫助。也非常感謝實驗室的同學們，能幫助我解決在研究上遇到的問題。感謝這段時間大家的互相支持與幫助。

最後謝謝我的父母及朋友，在這研究生生活中關心我並給我鼓勵。



Contents

Chinese Abstract	i
English Abstract	ii
Acknowledgement	iii
Contents	iv
List of Tables	vii
List of Figures	viii
1 Introduction	1
2 Preliminaries	4
2.1 Conventional MIMO System Model	4
2.2 Spatio-Temporally Correlated Channel	5
2.2.1 Spatial-Correlated Channel Model	5
2.2.2 Block-Fading Scenario	6
2.3 Spatial Modulation	7
2.3.1 SM System Model	7
2.3.2 SM Signal Detection	9



3	Estimation of Time-Varying MIMO Channels	10
3.1	Pilot-Assisted Channel Estimation	11
3.2	Decision-Directed Channel Estimation	12
3.2.1	Least Squares Estimation	12
3.2.2	Recursive Least Squares Estimation	13
3.2.3	Least Mean Squares Estimation	15
3.3	Model-Based (MB) Channel Estimation	17
3.4	Simulation Results	18
4	Spatio-Temporal Correlation and Channel Estimation Error-Aware ML Detection	26
4.1	ML Detection With MB Channel Estimates	27
4.1.1	Universal MIMO Signal Detection	27
4.1.2	An Alternative Perspective on ML Detector Derivation	29
4.1.3	ML Spatial-Modulated Signal Detectors	30
	▶ M -PSK	31
	▶ M -QAM	31
4.1.4	Complexity-Aware Near-ML M -PSK SM Detector	31
4.2	ML Detection With DD Channel Estimates	33
4.2.1	ML Spatial-Modulated Signal Detectors	34
	▶ M -PSK	34
	▶ M -QAM	35
4.2.2	Complexity-Aware Near-ML M -PSK SM Detector	35
4.3	Simulation Results	36
5	Approximated Maximum-Likelihood MIMO Detection	43
5.1	Approximated ML Detection With MB Channel Estimates	43
5.1.1	Universal MIMO Signal Detection	43

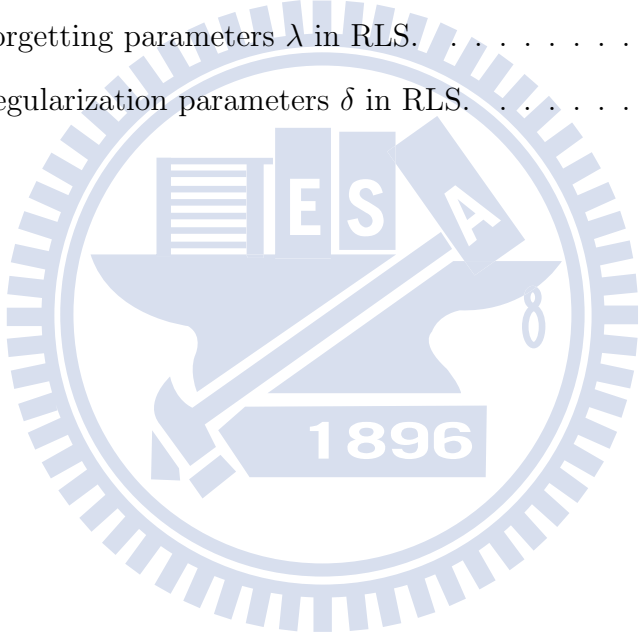
5.1.2	Complexity-Aware AML M -PSK SM Detector	45
5.1.3	Estimation of Channel Correlation	46
5.2	Approximated ML Detection With DD Channel Estimates	46
5.2.1	AML Spatial-Modulated Signal Detectors	46
5.2.2	Complexity-Aware AML M -PSK SM Detector	48
5.3	Simulation Results	48
6	Conclusion	59
	Bibliography	62



List of Tables

- 2.1 Signal mapping rules for 3-bit/transmission SM system 8

- 3.1 Simulation parameters 19
- 3.2 Values of forgetting parameters λ in RLS. 19
- 3.3 Values of regularization parameters δ in RLS. 20



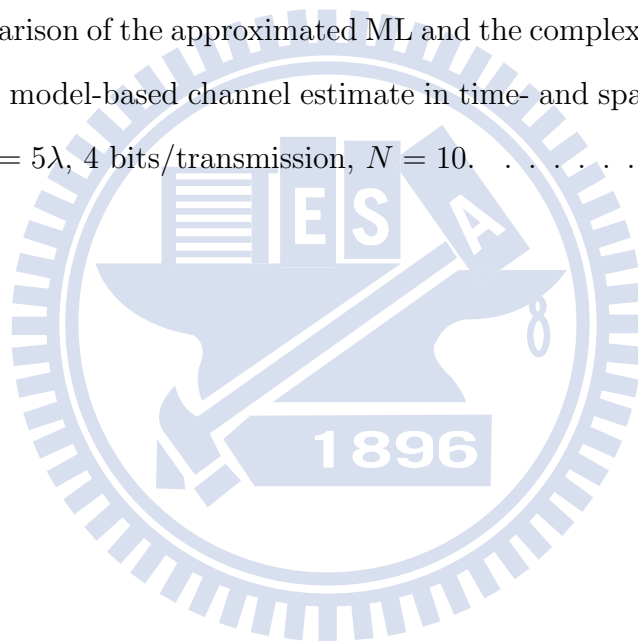
List of Figures

2.1	A MIMO system model.	5
2.2	An SM system model.	7
3.1	Periodical pilot signal inserion in transmit data.	10
3.2	BER of DD estimators with 3 bits/transmission; $N = 5$	20
3.3	Comparison of RLS and MB estimators with 3 bits/transmission; $N = 5$; $f_D T_s = 0.0222, 0.0370, 0.0519, 0.0667$	21
3.4	BER of DD estimator with 3 bits/transmission; $N = 40$	21
3.5	BER of MB estimators with 3 bits/transmission; $N = 40$; $f_D T_s = 0.0222, 0.0370, 0.0519$	22
3.6	BER of DD estimators with 6 bits/transmission, $N = 5$	22
3.7	Comparison of RLS and MB with 6 bits/transmission, $N = 5$; $f_D T_s =$ $0.0222, 0.0370, 0.0519, 0.0667$	23
3.8	MSE of RLS and LMS with 3 bits/transmission, $N = 5$	24
3.9	MSE of RLS and LMS 3 bits/transmission, $N = 40$	25
4.1	Performance of the various detectors with model-based channel estimate in time- and spatial- correlated channel; $\xi = 0.1\lambda$, 4 bits/transmission, $N = 10$ in 2×2 MIMO system.	38
4.2	Performance of the various detectors with model-based channel estimate in time- and spatial- correlated channel; $\xi = 1\lambda$, 4 bits/transmission, $N = 10$ in 2×2 MIMO system.	38

4.3	Performance of the various detectors with model-based channel estimate in time- and spatial- correlated channel; $\xi = 5\lambda$, 4 bits/transmission, $N = 10$ in 2×2 MIMO system.	39
4.4	Performance of the various detectors with model-based channel estimate in time- and spatial- correlated channel; $\xi = 1\lambda$, 8 bits/transmission, $N = 10$ in 2×2 MIMO system.	39
4.5	Performance of the various detectors with model-based channel estimate in time- and spatial- correlated channel; $\xi = 5\lambda$, 8 bits/transmission, $N = 10$ in 2×2 MIMO system.	40
4.6	Performance of the various detectors with decision-directed channel estimate in time- and spatial- correlated channel; $\xi = 1\lambda$, 4 bits/transmission, $N = 10$ in 4×4 MIMO system.	40
4.7	Performance of the various detectors with decision-directed channel estimate in time- and spatial- correlated channel; $\xi = 5\lambda$, 4 bits/transmission, $N = 10$ in 4×4 MIMO system.	41
4.8	Performance of the various detectors with model-based channel estimate in time- and spatial- correlated channel; $\xi = 0.1\lambda$, 4 bits/transmission, $N = 10$ in 4×4 SM MIMO system.	41
4.9	Performance of the various detectors with model-based channel estimate in time- and spatial- correlated channel; $\xi = 1\lambda$, 4 bits/transmission, $N = 10$ in 4×4 SM MIMO system.	42
5.1	BER performance comparison of the Approx. ML and mismatched detectors using decision-directed channel estimator in time-correlated channel; 3 bits/transmission, $N = 5$	50
5.2	Performance of various detectors with decision-directed channel estimate in time-correlated channel; 3 bits/transmission, $N = 40$	50

5.3	BER of Approx. ML and mismatched detectors using decision-directed channel estimate in channel with time correlation only; 6 bits/transmission, $N = 5$	51
5.4	BER comparison of the Approx. ML and mismatched detectors using decision-directed channel estimator in channel with time-spatial correlation; $\xi = 1\lambda$, 3 bits/transmission, $N = 5$	52
5.5	BER comparison of the Approx. ML and mismatched detectors using decision-directed channel estimator in channel with time-spatial correlation; $\xi = 5\lambda$, 3 bits/transmission, $N = 5$	52
5.6	Performance of the various detectors with model-based channel estimate in time- and spatial- correlated channel; $\xi = 0.1\lambda$, 4 bits/transmission, $N = 10$ in 4×4 SM MIMO system.	53
5.7	Performance of the various detectors with model-based channel estimate in time- and spatial- correlated channel; $\xi = 1\lambda$, 4 bits/transmission, $N = 10$ in 4×4 SM MIMO system.	53
5.8	Performance of the various detectors with decision-directed channel estimate in time- and spatial- correlated channel; $\xi = 1\lambda$, 4 bits/transmission, $N = 10$ in 4×4 SM MIMO system.	54
5.9	Performance of the various detectors with decision-directed channel estimate in time- and spatial- correlated channel; $\xi = 5\lambda$, 4 bits/transmission, $N = 10$ in 4×4 SM MIMO system.	54
5.10	BER comparison of the approximated ML and mismatched detectors using model-based channel estimator in channel with time-spatial correlation; $\xi = 0.1\lambda$, 4 bits/transmission, $N = 10$	55
5.11	Performance of the various detectors with model-based channel estimate in time- and spatial- correlated channel; $\xi = 1\lambda$, 4 bits/transmission, $N = 10$	56

5.12	Performance of the various detectors with model-based channel estimate in time- and spatial- correlated channel; $\xi = 5\lambda$, 4 bits/transmission, $N = 10$	56
5.13	BER comparison of the approximated ML and the complexity-reduced detector using model-based channel estimator in channel with time-spatial correlation; $\xi = 0.1\lambda$, 4 bits/transmission, $N = 10$	57
5.14	BER comparison of the approximated ML and the complexity-reduced detector with model-based channel estimate in time- and spatial- correlated channel; $\xi = 1\lambda$, 4 bits/transmission, $N = 10$	57
5.15	BER comparison of the approximated ML and the complexity-reduced detector with model-based channel estimate in time- and spatial- correlated channel; $\xi = 5\lambda$, 4 bits/transmission, $N = 10$	58



Chapter 1

Introduction

Spatial modulation (SM) is a promising multiple antennas based transmission scheme that induces no inter-(spatial) channel interference (ICI) and does not require timing synchronization amongst multiple spatial data streams. As it allows only one transmit antenna to be active in any one transmission interval [1], it needs a single radio frequency (RF) chain and exploit transmit antenna index for carrying extra information to enhance efficiency and capacity [2]. The low system complexity makes SM an attractive candidate for high rate transmissions. When it only exploits the transmit antenna index to carry information, SM degenerates to the so-called space-shift keying (SSK) [3, 4].

Performance assessment on multi-antenna based radio communication systems often assume that the channel state information (CSI) is perfectly known at the receiver. In practice, the CSI at the receiver (CSIR) is obtained by a pilot-assisted estimator. To minimize the overhead, pilot symbols are only sparsely and periodically inserted, CSIR is therefore inevitably imperfect, and tracking errors may sometimes result in serious performance degradation.

In many studies, the channel is assumed to be either time-invariant (static) within a frame consist of pilot block and data block [5]- [9]. This assumption yield poor performance valid for time-varying or correlated block-fading channels due to the change

of channel state within the time varying from the pilot block time to data block time in real world. In this thesis, we introduce some channel estimation schemes for use in time-varying block-faded channels. We release the assumption that the channel state estimated in pilot block is the same as that in data block. The first scheme is a decision-directed one which uses the detected signals of previous time block to update estimated channel coefficients. Since we insert pilot periodically in data stream, the CSI will update at least a frame time. This scheme has error floor in high SNR (signal to noise ratio) due to the error propagation of channel estimation.

To avoid error propagation problem, another scheme called model-based which use polynomials to fit the channel variation is proposed. Since the coefficients of the polynomials have to be solved for sufficient data, there is a process time (delay) in this method. Furthermore, we introduce some other adaptive channel estimations that are similar to decision-directed in conceptually. The first one is recursive least square (RLS) method whose objective is to minimize a weighted linear least squares cost function relating to the received signals. In this thesis, we will find that RLS method is a weighted version of the decision-directed channel estimation method. The other adaptive channel estimation method is least mean square (LMS) which converges slower but has lower complexity compared to RLS method.

The optimal detector method is the Maximum likelihood (ML) detector which often calls for exhaustive search over the entire set of possible transmitted symbol vectors. Due to noise and to the finite number of pilot symbols in a frame, the channel estimated is not perfect. The minimum Euclidean distance criterion is no longer the ML detection rule, but the statistic of the estimation/tracking error is known. There are lots of studies finding an ML detection metric with imperfect channel estimation [5]- [8], but many of them consider either time correlation only or spatial correlation only channel and assume that the pilot matrix and data matrix are in the same static channel.

We will derive a new ML detector structure that takes into account the CSIR error

and the transmission channel's time-spatial correlation, and a suboptimal ML detector whose complexity is lower than the proposed ML detector with near-ML performance is derived. We also derive another approximated version of ML detector whose complexity is less than the ML detector and performance is similar to it. Finally, we will compare the performance of the ML detector and approximated ML detector.

The rest of this thesis is organized as follows. In Chapter 2 we present the transceiver structure of a typical SM system along with spatial correlated channel models. In Chapter 3, we propose some adaptive time varying channel estimation methods and model-based method for SM systems and give simulated performance. In Chapter 4 and 5, we derive the detect metric that take time-spatial correlation of channel and imperfect CSI into account with exact and approximated versions respectively. Our main contributions are summarized in Chapter 6.

The following notations are used throughout the thesis: upper case bold symbols denote matrices and lower case bold symbols denote vectors. \mathbf{I}_N is a $N \times N$ identity matrix. $(\cdot)^T, (\cdot)^H$, and $(\cdot)^\dagger$ represent the transpose, conjugate transpose, and pseudo-inverse of the enclosed items, respectively. $(\cdot)^{-1}$ denotes the inverse of matrix. $\text{vec}(\cdot)$ is the operator that forms one tall vector by stacking columns of a matrix. While $\mathbb{E}\{\cdot\}$, $|\cdot|$, and $\|\cdot\|_F$ denote the expectation, absolute value, and Frobenius norm of the enclosed items, respectively, \otimes denotes the Kronecker product, and \odot denotes the Hadamard product. $(\cdot)_i$ and $[\cdot]_{ij}$ respectively denote the i th row and (i, j) th element of the enclosed matrix.

Chapter 2

Preliminaries

2.1 Conventional MIMO System Model

We consider a MIMO system with N_T transmit and N_R receive antennas and assume a block-fading scenario where the MIMO channel remains static within a block of B transmissions but varies from block to block. Thus, we treat the system block-wise and express the received signal at block k as

$$\mathbf{Y}(k) \stackrel{def}{=} [\mathbf{y}_1(k), \dots, \mathbf{y}_{N_R}(k)] = \mathbf{H}(k)\mathbf{X}(k) + \mathbf{Z}(k) \quad (2.1)$$

where $\mathbf{H}(k) = [\mathbf{h}_1(k), \dots, \mathbf{h}_{N_T}(k)] \stackrel{def}{=} [h_{ij}(k)]$ is the $N_R \times N_T$ wide-sense stationary MIMO channel, $\mathbf{X}(k) = [\mathbf{x}_1(k), \dots, \mathbf{x}_B(k)]$ the data matrix of size $N_T \times B$ ($B \geq N_T$), and the entries of noise $\mathbf{Z}(k)$ are i.i.d. $\mathcal{CN}(0, \sigma_z^2)$. This system is depicted in Fig. 2.1.

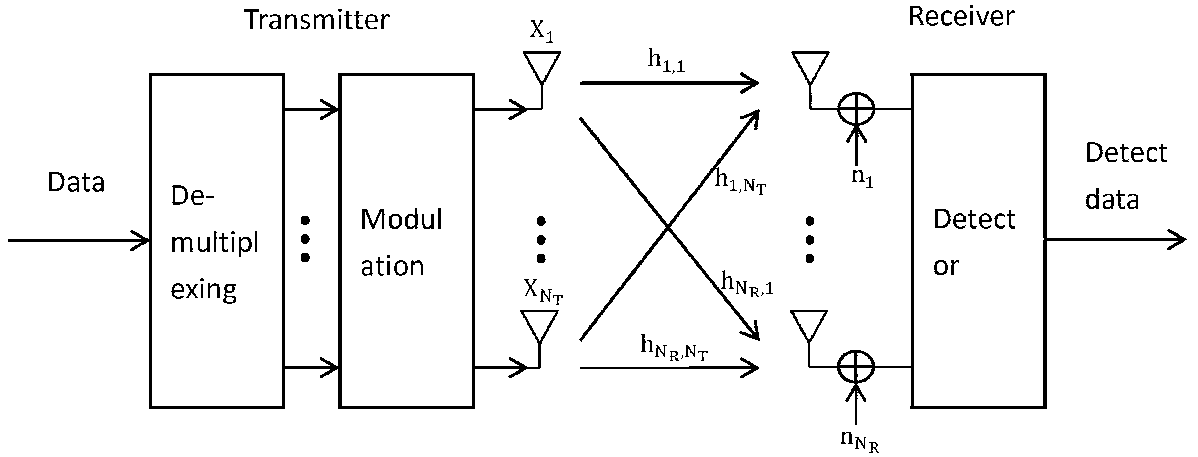


Figure 2.1: A MIMO system model.

2.2 Spatio-Temporally Correlated Channel

2.2.1 Spatial-Correlated Channel Model

Let $\Phi = \mathbb{E} \{ \text{vec}(\mathbf{H}(k)) \text{vec}^H(\mathbf{H}(k)) \}$ be the spatial correlation matrix of $\text{vec}(\mathbf{H}(k))$ that specifies the $(N_R N_T)^2$ mutual correlation coefficients between all channel entries. For instance, the spatial correlation matrix of a 2×2 channel can be described as

$$\Phi = \begin{bmatrix} 1 & r & t & s_1 \\ r^* & 1 & s_2 & t \\ t^* & s_2^* & 1 & r \\ s_1^* & t^* & r^* & 1 \end{bmatrix}, \quad (2.2)$$

where t and r are respectively transmit and receive antenna correlation coefficients and $s_1 \stackrel{\text{def}}{=} \mathbb{E}\{h_{11}(k)h_{22}^*(k)\}$ and $s_2 \stackrel{\text{def}}{=} \mathbb{E}\{h_{21}(k)h_{12}^*(k)\}$ are cross-channel correlation. Therefore, we may model the spatial-correlated Rayleigh fading channel as

$$\text{vec}(\mathbf{H}(k)) = \Phi^{\frac{1}{2}} \text{vec}(\mathbf{H}_w(k)), \quad (2.3)$$

where $\mathbf{H}_w(k)$ is an $N_R \times N_T$ spatially white (while may or may not be temporally correlated) complex Gaussian matrix with zero mean and unit variance.

As pointed out in [10] and [11], if at both the transmitter and receiver sides are locally of rich scatterers, the statistics at both sides is assumed separable. In such case, the spatial channel can be modeled by the famous Kronecker Model [12]:

$$\mathbf{H}(k) = \mathbf{\Phi}_R^{\frac{1}{2}} \mathbf{H}_w(k) \mathbf{\Phi}_T^{\frac{1}{2}}, \quad (2.4)$$

where the correlation matrix $\mathbf{\Phi}$ has been reduced to

$$\mathbf{\Phi} = \mathbf{\Phi}_T \otimes \mathbf{\Phi}_R, \quad (2.5)$$

the Kronecker product of the spatial correlation matrix of the transmitter side $\mathbf{\Phi}_T$ and that of receiver side $\mathbf{\Phi}_R$, where $\text{tr}(\mathbf{\Phi}_T) \mathbf{\Phi}_T \stackrel{\text{def}}{=} \mathbb{E}\{\mathbf{H}^H(k) \mathbf{H}(k)\}$ and $\text{tr}(\mathbf{\Phi}_R) \mathbf{\Phi}_R \stackrel{\text{def}}{=} \mathbb{E}\{\mathbf{H}(k) \mathbf{H}^H(k)\}$. With transmit and receive antennas being arranged into two uniform linear arrays (ULAs), [10] suggests that channel spatial correlation

$$\rho_S(i - m, j - n) \equiv \mathbb{E}\{h_{ij}(k) h_{mn}^*(k)\} = [\mathbf{\Phi}]_{(j-1)N_R+i, (n-1)N_R+m} = [\mathbf{\Phi}_T]_{nj} [\mathbf{\Phi}_R]_{im}. \quad (2.6)$$

The aforementioned correlation characteristics is adopted throughout this work for deriving channel estimators and signal detectors.

2.2.2 Block-Fading Scenario

On the other hand, while the channel is assumed to vary from block to block and remain unchanged in each block of B transmissions, the temporal correlation between blocks follows [10]

$$\mathbb{E}\{h_{ij}(k) h_{mn}^*(\ell)\} = \rho_S(i - m, j - n) \cdot \rho_T(k - \ell) \quad (2.7)$$

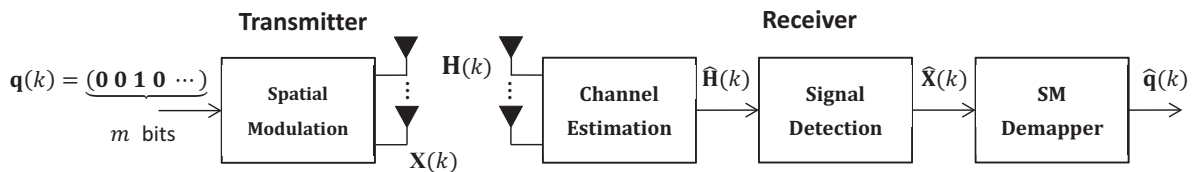


Figure 2.2: An SM system model.

with $\rho_T(k - \ell) \equiv \mathbb{E}\{h_{ij}(k)h_{ij}^*(\ell)\}$ denoting the channel correlation in time. As will be seen in the ensuing chapters, the proposed ML detectors require the information about spatio-temporal correlation. In addition to the scenario where such correlation values are well-known, we also consider cases when they are needed to be estimated prior to the detection.

2.3 Spatial Modulation

Despite the fact that spatial multiplexing (or BLAST) is widely used for MIMO systems, it suffers from significant ICI at the receiver. This makes signal detection algorithms of high complexity. Spatial modulation (SM) is a promising multi-antenna transmission scheme that eliminates ICI and does not require timing synchronization amongst transmission antennas. Since SM allows only one active transmit antenna at a time [1], it only requires a single RF chain. While the single-antenna limitation may seem to avoid ICI at the cost of data rate reduction, extra information is conveyed with the selection of transmit antenna and thus spectral efficiency can be retained [2].

2.3.1 SM System Model

Spatial modulation maps a block of information bits to: i) a symbol chosen from the constellation; ii) a transmit antenna that sends the symbol chosen. An m -bit/transmission SM system can be realized by partitioning the data bits into groups of $m = \log_2(MN_T)$ bits of which the first $\log_2 N_T$ bits represent the index of the transmit antenna to be

Table 2.1: Signal mapping rules for 3-bit/transmission SM system

Input bits	Mapping 1		Mapping 2	
	Tx antenna	Tx symbol	Tx antenna	Tx symbol
000	Ant. 1	+1	Ant. 1	$\exp(j\frac{\pi}{4})$
001	Ant. 1	-1	Ant. 1	$\exp(j\frac{3\pi}{4})$
010	Ant. 2	+1	Ant. 1	$\exp(j\frac{5\pi}{4})$
011	Ant. 2	-1	Ant. 1	$\exp(j\frac{7\pi}{4})$
100	Ant. 3	+1	Ant. 2	$\exp(j\frac{\pi}{4})$
101	Ant. 3	-1	Ant. 2	$\exp(j\frac{3\pi}{4})$
110	Ant. 4	+1	Ant. 2	$\exp(j\frac{5\pi}{4})$
111	Ant. 4	-1	Ant. 2	$\exp(j\frac{7\pi}{4})$

activated and the rest correspond to an element in \mathcal{A}_M , a constellation of size M . They as a whole constitute an SM symbol. An SM model is depicted in Fig. 2.2. Since only one transmit antenna is active at each transmission, $\mathbf{X}(k)$ has only one nonzero element in each column and the average transmission power is

$$E_s \stackrel{def}{=} \frac{1}{B} \mathbb{E} \{ \|\mathbf{X}(k)\|_F^2 \} = \frac{1}{B} \mathbb{E} \{ \text{tr} (\mathbf{X}(k)\mathbf{X}^H(k)) \}, \quad (2.8)$$

where E_s is equivalent to the average power of \mathcal{A}_M . Two mapping rules for the 3-bit/transmission SM system using BPSK or QPSK constellations with $E_s = 1$ are exemplified in Table 2.1. Therefore, for $j = 1, \dots, B$, the received signal at the j th symbol time of block k can be alternatively expressed as

$$\mathbf{y}_j(k) = \mathbf{h}_{\ell_j}(k)s_j(k) + \mathbf{z}_j, \quad (2.9)$$

where $\ell_j \equiv \ell_j(k)$ is the active transmit antenna index and $\mathbf{x}_j(k) = [0, \dots, 0, x_{\ell_j}(k), 0, \dots, 0]^T$ with the ℓ_j th entry $x_{\ell_j}(k) \stackrel{def}{=} s_j(k) \in \mathcal{A}_M$.

2.3.2 SM Signal Detection

Due to the fact that only one antenna is active at a time, maximum likelihood (ML) detector can be employed without too much computation effort. With the assumption of full CSI at the receiver (CSIR) and equally likely bit outcomes, ML detector aims to maximizing [15]

$$P(\mathbf{Y}(k)|\mathbf{H}(k), \mathbf{X}(k)) = (\pi\sigma_z^2)^{-N_R} \exp\left(-\frac{1}{\sigma_z^2} \|\mathbf{Y}(k) - \mathbf{H}(k)\mathbf{X}(k)\|_F^2\right), \quad (2.10)$$

which requires exhaustively searches over all possible transmit antenna index-constellation point pairs. Specifically, the decomposition into single-stream detection, $\forall j$,

$$\left(\hat{\ell}_j(k), \hat{s}_j(k)\right) = \arg \max_{\mathbf{x}} P(\mathbf{y}_j(k)|\mathbf{H}(k), \mathbf{x}) \quad (2.11)$$

$$= \arg \min_{(s,\ell) \in \mathcal{A}_M \times \{1, \dots, N_T\}} \|\mathbf{y}_j(k) - \mathbf{h}_\ell s\|^2 \quad (2.12)$$

which searches over a space of $\mathcal{O}(MN_T)$, is possible. Nevertheless, in the real-world scenario, it is impossible to obtain exact CSI which is available only when the pilot energy is infinitely large. In the ensuing chapters, we first develop some channel estimators and propose signal detectors in the presence of channel estimation error suitable for MIMO or particularly SM system.

Chapter 3

Estimation of Time-Varying MIMO Channels

In this chapter, we first introduce the conventional channel estimation schemes with the aid of pilot blocks. Subsequently, methods that help reduce training overhead are also given. Among them, three adaptive estimators that treat previous detected data as pilots and an estimator which models channel variations in time using polynomials are introduced. The MIMO signal frame structure used through the thesis is depicted in Fig. 3.1, where a pilot signal block is inserted as preamble into each frame. Specifically, a frame of N blocks is consisted of one pilot block followed by $N - 1$ data blocks and therefore occupies NB symbol times. The value of N , or equivalently the sparsity of pilots, relies highly on the rapidity of channel change in time.



Figure 3.1: Periodical pilot signal inserion in transmit data.

3.1 Pilot-Assisted Channel Estimation

Let the channel coefficients be obtained at the training block k_p by transmitting $N_T \times B$ pilot matrix $\mathbf{X}(k_p) = \mathbf{X}_P$ which is known to both sides. The received signal can be written as

$$\mathbf{Y}(k_p) = \mathbf{H}(k_p)\mathbf{X}_P + \mathbf{Z}(k_p), \quad (3.1)$$

where \mathbf{X}_p is a constant matrix with average power denoted by

$$E_P \stackrel{def}{=} \frac{1}{B} \|\mathbf{X}_P\|_F^2. \quad (3.2)$$

Without loss of generality, we may assume throughout this work that \mathbf{X}_p is full-rank with only one nonzero element on each column to enable its usage on the SM systems. Two conventional estimators are provided as follows.

In the absence of channel and noise statistics, a simple least squares (LS) estimator, which minimizes $\|\mathbf{Y}(k_p) - \mathbf{H}(k_p)\mathbf{X}(k_p)\|_F^2$, may be applied using the received pilot, i.e.,

$$\hat{\mathbf{H}}_{\text{LS}}(k_p) = \mathbf{Y}(k_p)\mathbf{X}_P^\dagger = \mathbf{H}(k_p) + \mathbf{Z}(k_p)\mathbf{X}_P^\dagger \quad (3.3)$$

where $\mathbf{A}^\dagger \stackrel{def}{=} \mathbf{A}^H(\mathbf{A}\mathbf{A}^H)^{-1}$. The fact that LS estimator neglects channel statistics may lead to significant noise power enhancement and thus serious channel equalization performance degradation. To deal with such potential problem, we alternatively aim to find an \mathbf{F} that minimizes the mean square error (MSE) $\mathbb{E} \{ \|\mathbf{Y}(k_p)\mathbf{F} - \mathbf{H}(k_p)\|_F^2 \}$. Therefore, we have $\hat{\mathbf{H}}_{\text{MMSE}}(k_p) \stackrel{def}{=} \mathbf{Y}(k_p)\mathbf{F}$ where

$$\mathbf{F} = (\sigma_z^2 N_R \mathbf{I}_B + \mathbf{X}_P^H \Phi_T \mathbf{X}_P)^{-1} \mathbf{X}_P^H \Phi_T. \quad (3.4)$$

In the rest of this chapter, $\hat{\mathbf{H}}_{\text{LS}}(k_p)$ or $\hat{\mathbf{H}}_{\text{MMSE}}(k_p)$ are exploited as reliable initial guess for the adaptive channel estimation methods.

3.2 Decision-Directed Channel Estimation

In this section, we refer to the decision-directed (DD) channel estimation as the scheme that treats previous detected data blocks as known pilot and updates the estimates sequentially, while detecting data using the CSI estimated in the previous block; see Chapter 4 and Chapter 5. Just as all other DD algorithms, the proposed DD channel estimator for SM systems suffers from error propagation. To mitigate the error propagation problem, channel estimates are entirely renewed at each pilot block $k_p + sN$, $s \in \mathbb{N}$.

3.2.1 Least Squares Estimation

Due to the nature of SM signal that only one element in each column of $\hat{\mathbf{X}}(k)$, the detected block k , should be nonzero, it is likely that not all channel vectors $\mathbf{h}_\ell(k)$'s are updated at each block instance. Nevertheless, in the long run, all channel coefficients would be updated since the transmit antenna is selected uniformly. Assume for the moment that the detected data matrix $\hat{\mathbf{X}}(k)$ is full-rank. Let $\hat{\mathbf{X}}(k_p + sN) = \mathbf{X}_P$. By treating $\hat{\mathbf{X}}(k)$ as pilot the LS estimate of $\mathbf{H}(k)$ is obtainable, i.e.,

$$\hat{\mathbf{H}}(k) = \mathbf{Y}(k)\hat{\mathbf{X}}^\dagger(k) \quad (3.5)$$

for $k_p + sN < k < k_p + (s + 1)N$. However, due to the fact that $\mathbf{X}(k)$ or $\hat{\mathbf{X}}(k)$ is not full-rank most of the time, we let $\hat{\mathbf{H}}(k) = [\hat{\mathbf{h}}_1(k), \dots, \hat{\mathbf{h}}_{N_T}(k)]$ and denote by $\mathbf{H}[\mathcal{L}](k)$ the truncated $\mathbf{H}(k)$ by eliminating the columns not specified in the set \mathcal{L} . As a result, we have

$$\hat{\mathbf{H}}[\hat{\mathcal{L}}(k)](k) = \mathbf{Y}(k)\bar{\mathbf{X}}^\dagger(k),$$

where $\hat{\mathcal{L}}(k) \stackrel{def}{=} \{\hat{\ell}_1(k), \dots, \hat{\ell}_B(k)\}$ and $\bar{\mathbf{X}}(k)$ is the truncated $\hat{\mathbf{X}}(k)$ with its all-zero rows removed. On the other hand, the columns not updated in this block are kept unchanged as the previous block to avoid the rank insufficient problem as well, i.e.,

$$\hat{\mathbf{H}}[\mathbb{L} \setminus \hat{\mathcal{L}}(k)](k) = \hat{\mathbf{H}}[\mathbb{L} \setminus \hat{\mathcal{L}}(k)](k-1), \quad (3.6)$$

where $\mathbb{L} \stackrel{def}{=} \{1, \dots, N_T\}$.

Inspired by the fact that a channel vector may not be updated at every block time and thus its previous estimate must be used to retain the integrity, a natural generalization is to include the estimates of the whole channel of several previous blocks. Such inclusion ameliorates the performance degradation error propagation has brought about. In the subsequent subsections, two adaptive methods that not only improve performance but also save the heavy computation of matrix inversion are given.

3.2.2 Recursive Least Squares Estimation

To make channel estimation robust and computationally efficient, the LS criterion is replaced by the recursive least squares (RLS) estimation which in addition eliminates the need to perform matrix inversions. Specifically, we are interested in solving

$$\hat{\mathbf{H}}(k) = \arg \min_{\tilde{\mathbf{H}}} \left\{ \|\mathbf{Y}(k) - \tilde{\mathbf{H}}\hat{\mathbf{X}}(k)\|_F^2 + \sum_{i=k_p+sN+1}^{k-1} \lambda^{k-i} \|\mathbf{Y}(i) - \tilde{\mathbf{H}}\hat{\mathbf{X}}(i)\|_F^2 + \delta \lambda^{k-k_p-sN} \|\tilde{\mathbf{H}}\|_F^2 \right\} \quad (3.7)$$

for $k_p + sN < k < k_p + (s+1)N$, $s \in \mathbb{N}$, where the first two terms comprise the sum of weighted error squares and the last is a regularizing term with δ being the regularization parameter. Moreover, $\lambda \in (0, 1)$ can be treated as a forgetting factor. By differentiation, we have

$$\hat{\mathbf{H}}(k) = \mathbf{Z}(k)\mathbf{P}^{-1}(k), \quad (3.8)$$

where $\mathbf{Z}(k) = \sum_{i=k_p+sN+1}^k \lambda^{k-i} \mathbf{Y}(i) \hat{\mathbf{X}}^H(i)$ and

$$\mathbf{P}(k) = \text{Diag} \left(\sum_{i=k_p+sN+1}^k \lambda^{k-i} \|\hat{\mathbf{X}}_1(i)\|_F^2, \dots, \sum_{i=k_p+sN+1}^k \lambda^{k-i} \|\hat{\mathbf{X}}_{N_T}(i)\|_F^2 \right) + \delta \lambda^{k-k_p-sN} \mathbf{I}_{N_T} \quad (3.9)$$

with $\hat{\mathbf{X}}_r(i)$ being the r th row of $\hat{\mathbf{X}}(i)$. The recursion formulae for (3.8) are readily derivable [16]:

$$\mathbf{P}^{-1}(k) = \lambda^{-1} \mathbf{P}^{-1}(k-1) (\mathbf{I}_{N_T} - \mathbf{C}(k) \mathbf{K}(k)) \quad (3.10)$$

$$\mathbf{Z}(k) = \lambda \mathbf{Z}(k-1) + \mathbf{Y}(k) \hat{\mathbf{X}}^H(k) \quad (3.11)$$

where

$$\mathbf{C}(k) = \text{Diag} \left(\|\hat{\mathbf{X}}_1(k)\|_F, \dots, \|\hat{\mathbf{X}}_{N_T}(k)\|_F \right) = \left(\hat{\mathbf{X}}(k) \hat{\mathbf{X}}^H(k) \odot \mathbf{I}_{N_T} \right)^{\frac{1}{2}} \quad (3.12)$$

$$\mathbf{K}(k) = \lambda^{-1} \left(\mathbf{I}_{N_T} + \lambda^{-1} \mathbf{C}^H(k) \mathbf{P}^{-1}(k-1) \mathbf{C}(k) \right)^{-1} \mathbf{C}^H(k) \mathbf{P}^{-1}(k-1). \quad (3.13)$$

Finally, due to the fact that $\mathbf{C}(k)$ and $\mathbf{P}(k)$ are diagonal, a matrix inversion-free version of (3.8) is derived:

$$\begin{aligned} \hat{\mathbf{H}}(k) &= \lambda \mathbf{Z}(k-1) \mathbf{P}^{-1}(k) + \mathbf{Y}(k) \hat{\mathbf{X}}^H(k) \mathbf{P}(k)^{-1} \\ &= \hat{\mathbf{H}}(k-1) (\mathbf{I} - \mathbf{C}(k) \mathbf{K}(k)) + \mathbf{Y}(k) \hat{\mathbf{X}}^H(k) \mathbf{P}^{-1}(k). \end{aligned} \quad (3.14)$$

The RLS estimation algorithm is summarized in Algorithm 1.

To conclude this subsection, we observe that $\mathbf{C}(k) \mathbf{K}(k)$ is also diagonal and with its ι th diagonal element being zero if $\iota \in \mathbb{L} \setminus \hat{\mathcal{L}}(k)$. Therefore, columns of $\hat{\mathbf{H}}(k)$ with indices belong to $\iota \in \mathbb{L} \setminus \hat{\mathcal{L}}(k)$ will not be updated by the new information obtained from $\mathbf{Y}(k)$ but maintained only by the old detected data blocks, while the rest of the columns are updated by the combination of the new and old information. On the other hand,

Algorithm 1 DD RLS Channel Estimation

```
1: (Initialization) Initialize some  $\lambda$  and  $\delta$ .
2: repeat
3:   if  $k = k_p + sN$  then
4:      $\hat{\mathbf{H}}(k) := \hat{\mathbf{H}}_{\text{LS}}(k)$  or  $\hat{\mathbf{H}}_{\text{MMSE}}(k)$ ;
5:      $\mathbf{P}^{-1}(k) := \delta^{-1}\mathbf{I}_{N_T}$ .
6:   else
7:      $k := k + 1$ ;
8:      $\tilde{\mathbf{X}}(k) := \arg \min_{[\tilde{\mathbf{x}}]_{ij} \in \mathcal{A}_M \cup \{0\}} P(\mathbf{Y}(k) | \tilde{\mathbf{X}}, \hat{\mathbf{H}}(k-1))$ ;
9:      $\mathbf{C}(k) := \left( \left( \tilde{\mathbf{X}}(k) \tilde{\mathbf{X}}^H(k) \right) \odot \mathbf{I}_{N_T} \right)^{\frac{1}{2}}$ 
10:     $\mathbf{K}(k) := \lambda^{-1} \left( \mathbf{I}_{N_T} + \lambda^{-1} \mathbf{C}^H(k) \mathbf{P}^{-1}(k-1) \mathbf{C}(k) \right)^{-1} \mathbf{C}^H(k) \mathbf{P}^{-1}(k-1)$ ;
11:     $\mathbf{P}^{-1}(k) := \lambda^{-1} \mathbf{P}^{-1}(k-1) \left( \mathbf{I}_{N_T} - \mathbf{C}(k) \mathbf{K}(k) \right)$ ;
12:     $\hat{\mathbf{H}}(k) := \hat{\mathbf{H}}(k-1) \left( \mathbf{I} - \mathbf{C}(k) \mathbf{K}(k) \right) + \mathbf{Y}(k) \tilde{\mathbf{X}}^H(k) \mathbf{P}^{-1}(k)$ .
13:   end if
14: until Transmission is ended.
```

scalars λ and δ are determined empirically by the system signal-to-noise ratio (SNR) to attain better performance. Specifically, they are roughly inverse proportional to SNR because the detected data may be very unreliable in the low SNR regime. In this way, the channel estimates of the current block is more dependent on the previous blocks even for the channel vectors indexed $\hat{\mathcal{L}}(k)$. On the contrary, (3.14) approaches the LS estimator for high SNRs for its forgetfulness of the past.

3.2.3 Least Mean Squares Estimation

While previous two DD estimators originate from the LS criterion, in this subsection we consider an adaptive estimator that aims to minimize MSE. Specifically, the least mean squares (LMS) estimate [16]

$$\hat{\mathbf{H}}(k) = \hat{\mathbf{H}}(k-1) - \frac{1}{2} \mu \nabla \mathbf{J}(\hat{\mathbf{H}}(k-1)) \quad (3.15)$$

tracks the minimum of

$$\mathbf{J}(\tilde{\mathbf{H}}) = \mathbb{E} \left\{ \|\mathbf{Y}(k) - \tilde{\mathbf{H}} \hat{\mathbf{X}}(k)\|^2 \right\} \quad (3.16)$$

Algorithm 2 DD LMS Channel Estimation

```

1: (Initialization) Initialize some  $\mu$ .
2: repeat
3:   if  $k = k_p + sN$  then
4:      $\hat{\mathbf{H}}(k) := \hat{\mathbf{H}}_{\text{LS}}(k)$  or  $\hat{\mathbf{H}}_{\text{MMSE}}(k)$ ;
5:   else
6:      $k := k + 1$ ;
7:      $\hat{\mathbf{X}}(k) := \arg \min_{[\tilde{\mathbf{X}}]_{ij} \in \mathcal{A}_M \cup \{0\}} P(\mathbf{Y}(k) | \tilde{\mathbf{X}}, \hat{\mathbf{H}}(k-1))$ ;
8:      $\hat{\mathbf{H}}(k) = \hat{\mathbf{H}}(k-1) \left( \mathbf{I}_{N_T} - \frac{1}{2} \mu \hat{\mathbf{X}}(k) \hat{\mathbf{X}}^H(k) \right) + \frac{1}{2} \mu \mathbf{Y}(k) \hat{\mathbf{X}}^H(k)$ .
9:   end if
10: until Transmission is ended.
  
```

along the gradient direction $\nabla \mathbf{J}(\hat{\mathbf{H}}(k-1))$ with updating step size μ , for $k_p + sN < k < k_p + (s+1)N$, $s \in \mathbb{N}$, where we may derive

$$\nabla \mathbf{J}(\hat{\mathbf{H}}(k-1)) = \hat{\mathbf{H}}(k-1) \hat{\mathbf{X}}(k) \hat{\mathbf{X}}(k)^H - \mathbf{Y}(k) \hat{\mathbf{X}}^H(k). \quad (3.17)$$

Consequently, the channel estimate can be updated via

$$\begin{aligned} \hat{\mathbf{H}}(k) &= \hat{\mathbf{H}}(k-1) - \frac{1}{2} \mu \left(\hat{\mathbf{H}}(k-1) \hat{\mathbf{X}}(k) \hat{\mathbf{X}}(k)^H - \mathbf{Y}(k) \hat{\mathbf{X}}^H(k) \right) \\ &= \hat{\mathbf{H}}(k-1) \left(\mathbf{I}_{N_T} - \frac{1}{2} \mu \hat{\mathbf{X}}(k) \hat{\mathbf{X}}^H(k) \right) + \frac{1}{2} \mu \mathbf{Y}(k) \hat{\mathbf{X}}^H(k) \end{aligned} \quad (3.18)$$

$$= \hat{\mathbf{H}}(k-1) \left(\mathbf{I}_{N_T} - \frac{1}{2} \mu \hat{\mathbf{X}}(k) \hat{\mathbf{X}}^H(k) \right) + \mathbf{Y}(k) \hat{\mathbf{X}}^\dagger(k) \left(\frac{1}{2} \mu \hat{\mathbf{X}}(k) \hat{\mathbf{X}}^H(k) \right). \quad (3.19)$$

The LMS estimation algorithm is summarized in Algorithm 2.

We can see from (3.19) that the estimated channel coefficients are updated by the linear combination of the last estimates $\hat{\mathbf{H}}(k-1)$ and the new ones $\mathbf{Y}(k) \hat{\mathbf{X}}^\dagger(k)$, the LS estimates obtained in Section 3.2.3, with a weighting factor of $\frac{1}{2} \mu \hat{\mathbf{X}}(k) \hat{\mathbf{X}}^H(k)$. It bears a similarity to the RLS estimator (3.14) in that they both take the past estimates into account to deal with the possibility that the newly detected data might not be reliable enough for channel estimation. In the next section, we introduce another estimator that does not produce any error propagation as that lies in DD algorithms.

3.3 Model-Based (MB) Channel Estimation

In this section, 2nd-order polynomials are utilized to capture the channel variation in time. Specifically, if the (i, j) th component of the channel can be modeled as

$$h_{ij}(k) = \alpha_{ij}(k)k^2 + \beta_{ij}(k)k + \gamma_{ij}(k) \quad (3.20)$$

where $\boldsymbol{\xi}_{ij}(k) \stackrel{\text{def}}{=}} [\alpha_{ij}(k), \beta_{ij}(k), \gamma_{ij}(k)]^T$ are the coefficients of the polynomial, $\mathbf{H}(k)$ is estimated once $\boldsymbol{\xi}_{ij}(k)$'s are obtained for all i and j , where $\boldsymbol{\xi}_{ij}(k)$'s are updated every 2 frames. Specifically, at block $k_p + 2N$, three pilot blocks at k_p , $k_p + N$, and $k_p + 2N$ are gathered to solve $\boldsymbol{\xi}_{ij}(k_p)$, and then $\boldsymbol{\xi}_{ij}(k_p + 2N)$ is solved with pilot blocks at $k_p + 2N$, $k_p + 3N$, and $k_p + 4N$; so on and so forth. Without loss of generality, we will assume $\mathbf{X}_P = E_P \mathbf{I}_{N_T}$ and $B = N_T$ throughout this work to avoid excessive notations.

Collecting received signals $\mathbf{Y}(k_p)$, $\mathbf{Y}(k_p + N)$, and $\mathbf{Y}(k_p + 2N)$

$$\tilde{\mathbf{y}}_{ij}(k_p) \stackrel{\text{def}}{=} \begin{bmatrix} y_{ij}(k_p) \\ y_{ij}(k_p + N) \\ y_{ij}(k_p + 2N) \end{bmatrix} = \begin{bmatrix} h_{ij}(k_p) \\ h_{ij}(k_p + N) \\ h_{ij}(k_p + 2N) \end{bmatrix} + \tilde{\mathbf{z}}_{ij}(k_p), \quad (3.21)$$

we may solve

$$\hat{\boldsymbol{\xi}}_{ij}(k_p) \stackrel{\text{def}}{=} \begin{bmatrix} \hat{\alpha}_{ij}(k_p) \\ \hat{\beta}_{ij}(k_p) \\ \hat{\gamma}_{ij}(k_p) \end{bmatrix} = \mathbf{T}^{-1}(k_p) \tilde{\mathbf{y}}_{ij}(k_p) \quad (3.22)$$

with

$$\mathbf{T}(k) \stackrel{\text{def}}{=} \begin{bmatrix} k^2 & k & 1 \\ (k + N)^2 & k + N & 1 \\ (k + 2N)^2 & k + 2N & 1 \end{bmatrix},$$

where $\tilde{\mathbf{z}}_{ij}(k_p) \sim \mathcal{CN}(\mathbf{0}, \sigma_k^2 \mathbf{I}_3)$. Finally, with (3.20), (3.22), and $\mathbf{t}(k) = [k^2, k, 1]^H$, the

channel estimates

$$\hat{h}_{ij}(k) = \mathbf{t}^H(k) \hat{\boldsymbol{\xi}}_{ij}(k_p) = \mathbf{t}^H(k) \mathbf{T}^{-1}(k_p) \tilde{\mathbf{y}}_{ij}(k_p) \quad (3.23)$$

at pilot blocks k_p and $k_p + N$ and data blocks $k \in \{k_p + 1, \dots, k_p + N - 1, k_p + N + 1, \dots, k_p + 2N - 1\}$ can be respectively retained and interpolated. While this approach avoids error propagation, the issue of long latency arises if the system is of low overhead (or long frame) and thus has to wait for a long time to amass three pilots. This may be even more serious if higher order polynomials are applied.

3.4 Simulation Results

In this section, the performance of aforementioned estimators are simulated. While frame structure shown in Fig. 3.1 is adopted, the pilot block at the beginning of each frame is assumed to be an identity matrix; thus, $B = N_T$. We consider the estimation of block-fading, spatially-uncorrelated 4×4 MIMO channels with SM signals, where the time variation follows the Jakes' model [17]. Specifically, time correlation is assumed to be

$$\rho_T(k - \ell) = J_0(2\pi f_D |t_1 - t_2| B T_s), \quad (3.24)$$

where f_D is the Doppler frequency. Throughout this section, 4- and 6-bit/transmission rate are respectively achieved with \mathcal{A}_M being BPSK and 16-QAM constellation, i.e., $M = 4$ and 16. Besides, frame size of 5 and 40 are used to investigate the effect of error propagation lies in the DD estimators. The rest of the simulation parameters are list in Table 3.1. While the performance of channel estimators are investigated through bit error rate (BER), canonical (or later called mismatched) detectors

$$\hat{\mathbf{X}} = \arg \min_{[\tilde{\mathbf{X}}]_{ij} \in \mathcal{A}_M \cup \{0\}} \|\mathbf{Y}(k) - \hat{\mathbf{H}}\tilde{\mathbf{X}}\|_F; \quad (3.25)$$

Table 3.1: Simulation parameters

<i>Parameters</i>	<i>Values</i>
Operating frequency	2 GHz
Symbol period	0.1 ms
Number of transmit antennas N_T	4
Number of receive antennas N_R	4
Block size B	4

Table 3.2: Values of forgetting parameters λ in RLS.

		SNR (dB)					
		0	4	8	12	16	20
$f_D T_s$	0.0222	0.6400	0.5120	0.4096	0.3277	0.0467	0.0280
	0.0370	0.5120	0.4096	0.3277	0.2621	0.0280	0.0168
	0.0519	0.4096	0.3277	0.2621	0.2097	0.0168	0.0101
	0.0667	0.3277	0.2621	0.2097	0.1678	0.0101	0.0060

which treat channel estimates as real channels are employed, where $\hat{\mathbf{H}} = \hat{\mathbf{H}}(k)$ for MB estimators and $\hat{\mathbf{H}}(k-1)$ for DD ones.

μ in LMS algorithm is 1.45.

In Fig. 3.2 and Fig. 3.4, we compared the BER of recursive least square (RLS) and LS both using decision-directed (DD) with 3 bits/transmission at different velocity and frame size are 5 and 40, respectively. As mentioned in Subsection 3.2.2 the RLS updated equation is similar to the LS updated equation. Both channel coefficients at next time index are the linear combination of channel coefficient at last time index and the received data in this time index.

In Fig. 3.3-3.5, we compared the BER of RLS, LMS and MB estimators with 3 bits/transmission and frame size 5 or 40 at different velocity. It can be seen from LMS estimator that channel coefficient at next time index are also the linear combination of channel coefficient at last time index and the received data this time index, but the weighting factor does not change with SNR. Therefore, even in high SNR, the channel is updated by the 'old' channel coefficients with certain ratio causing the poor performance than RLS. However, the benefit of LMS is low complexity compared to the RLS method. On the other hand, the performance of the MB estimator outperform the RLS estimator

Table 3.3: Values of regularization parameters δ in RLS.

SNR (dB)	0	4	8	12	16	20
δ	1000	0.0665	0.0186	0.0067	0.0026	0.0001

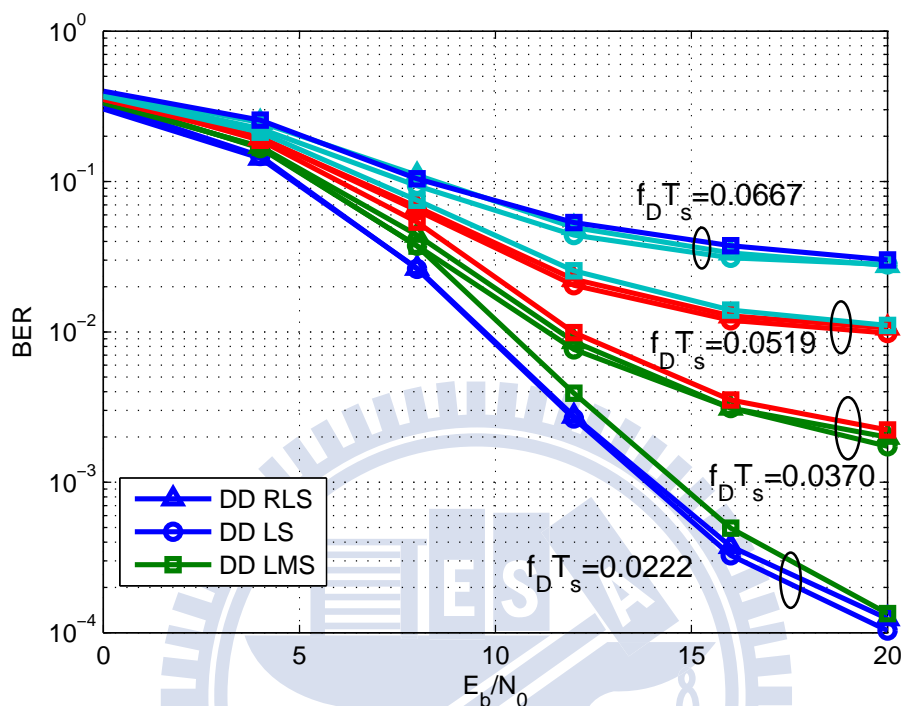


Figure 3.2: BER of DD estimators with 3 bits/transmission; $N = 5$.

and LMS estimator at frame size 5, but worse than them when the frame size become larger. This is because the polynomial order is too small to chase the channel variation if the frame size is too large. The MB estimator is sensitive to the change of the velocity. Fig. 3.6-3.7 is the simulation result of RLS, LS, LMS and MB estimator with 16-QAM and frame size is 5.

In Fig.3.8 and Fig.3.9, we compared the Mean square Error (MSE) of RLS and LMS at different SNR and different velocity. When the iterations number is large, both algorithm converge at low velocity. Both figure shows that the RLS algorithm have lower MSE than LMS algorithm, which explains the performance of LMS is poor than the RLS algorithm in Fig.3.8 and Fig.3.9. Furthermore, when the SNR is large, the MSE of these two algorithm get closer.

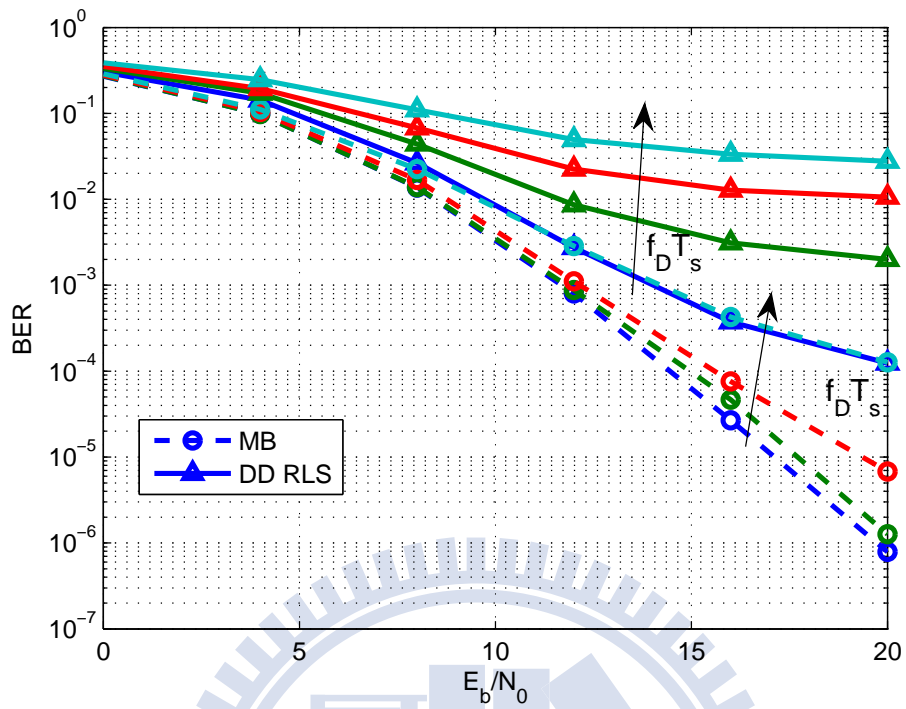


Figure 3.3: Comparison of RLS and MB estimators with 3 bits/transmission; $N = 5$; $f_D T_s = 0.0222, 0.0370, 0.0519, 0.0667$.

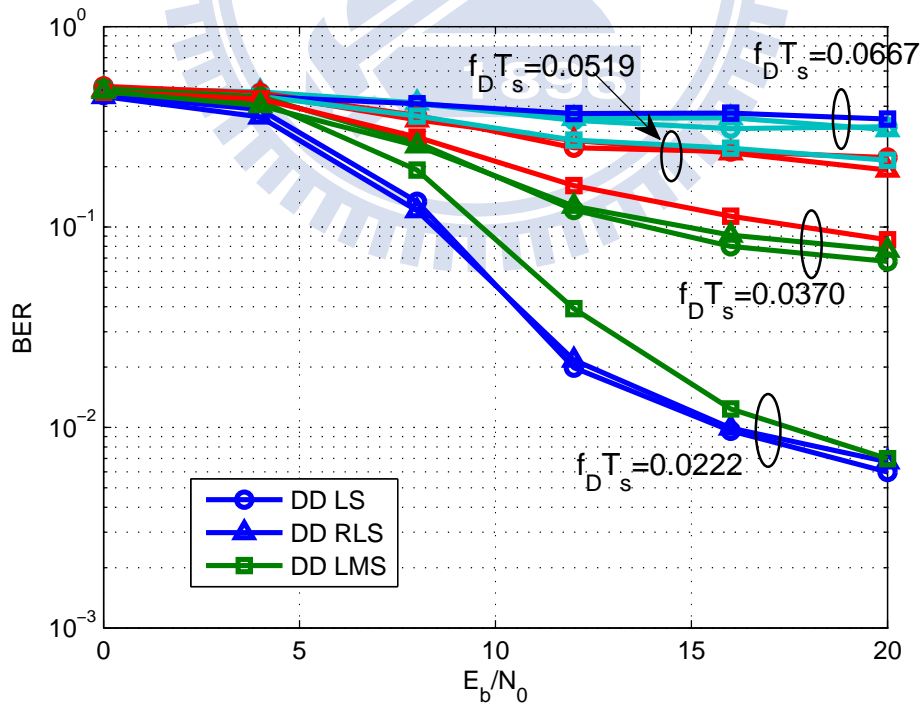


Figure 3.4: BER of DD estimator with 3 bits/transmission; $N = 40$.

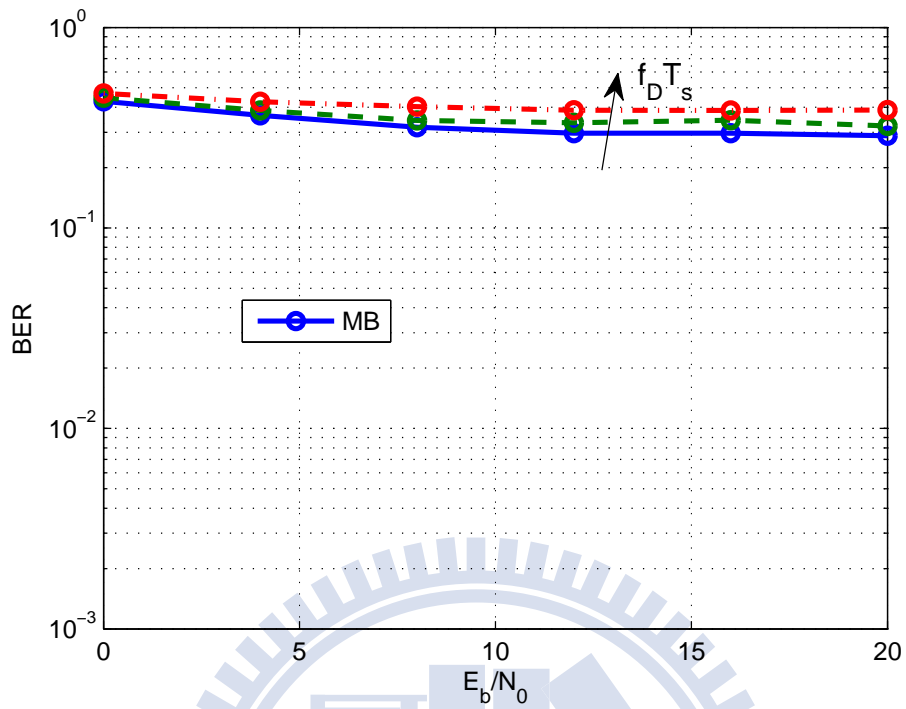


Figure 3.5: BER of MB estimators with 3 bits/transmission; $N = 40$; $f_D T_s = 0.0222, 0.0370, 0.0519$.

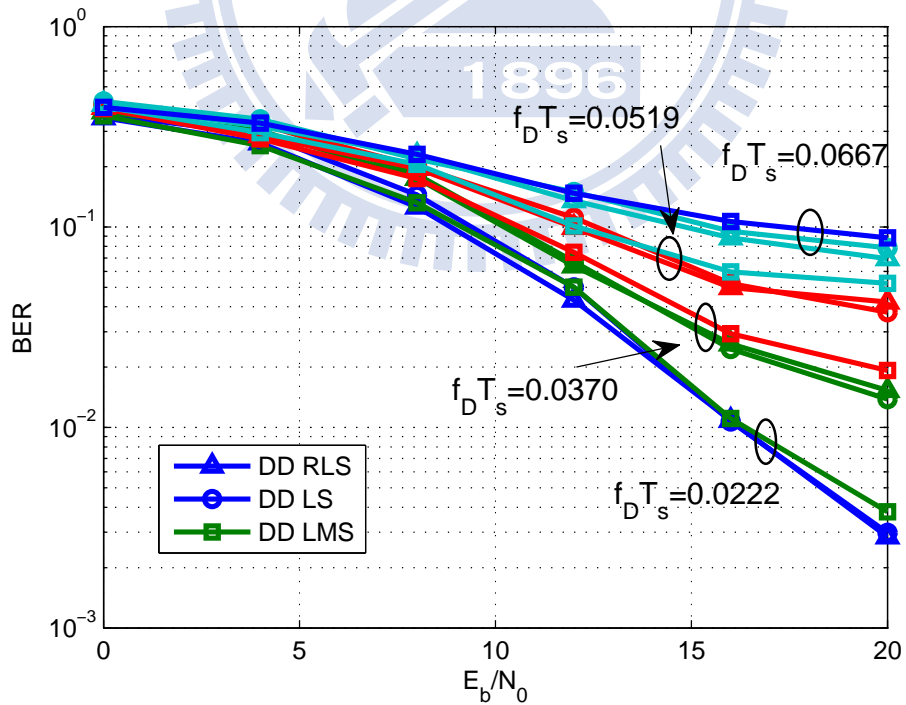


Figure 3.6: BER of DD estimators with 6 bits/transmission, $N = 5$.

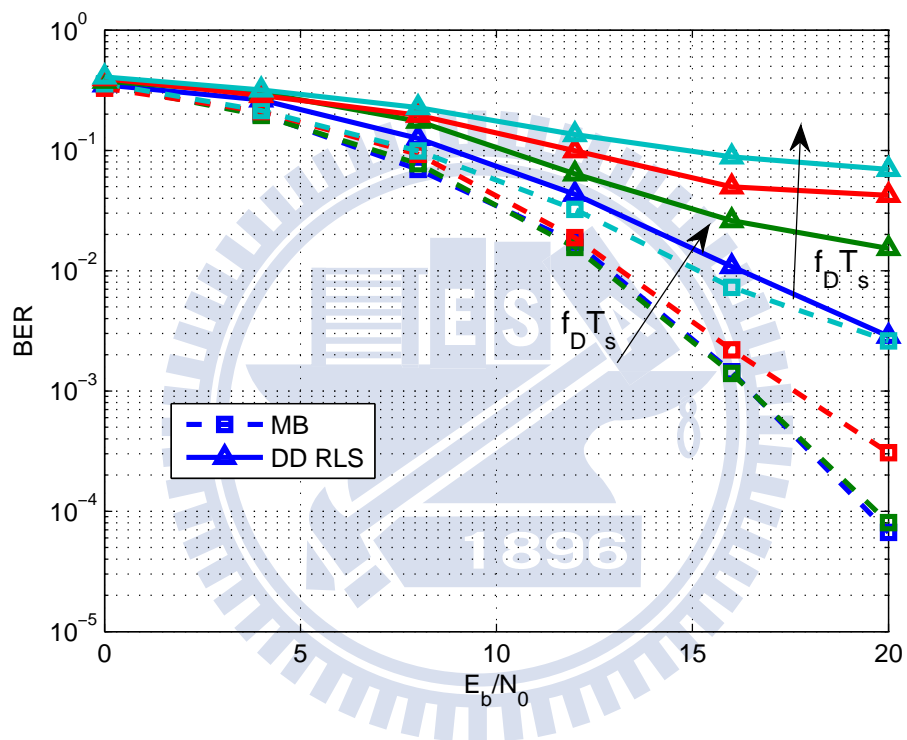


Figure 3.7: Comparison of RLS and MB with 6 bits/transmission, $N = 5$; $f_D T_s = 0.0222, 0.0370, 0.0519, 0.0667$.

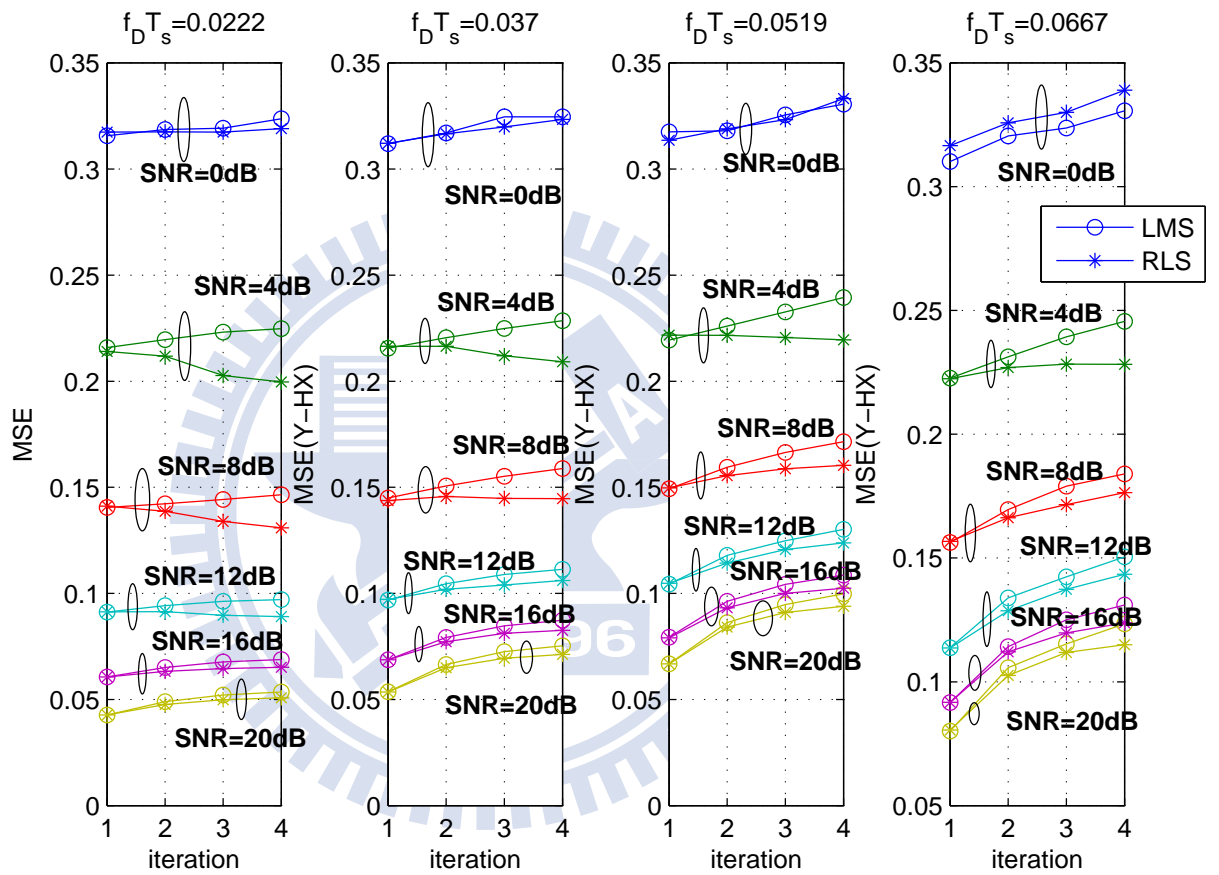


Figure 3.8: MSE of RLS and LMS with 3 bits/transmission, $N = 5$.

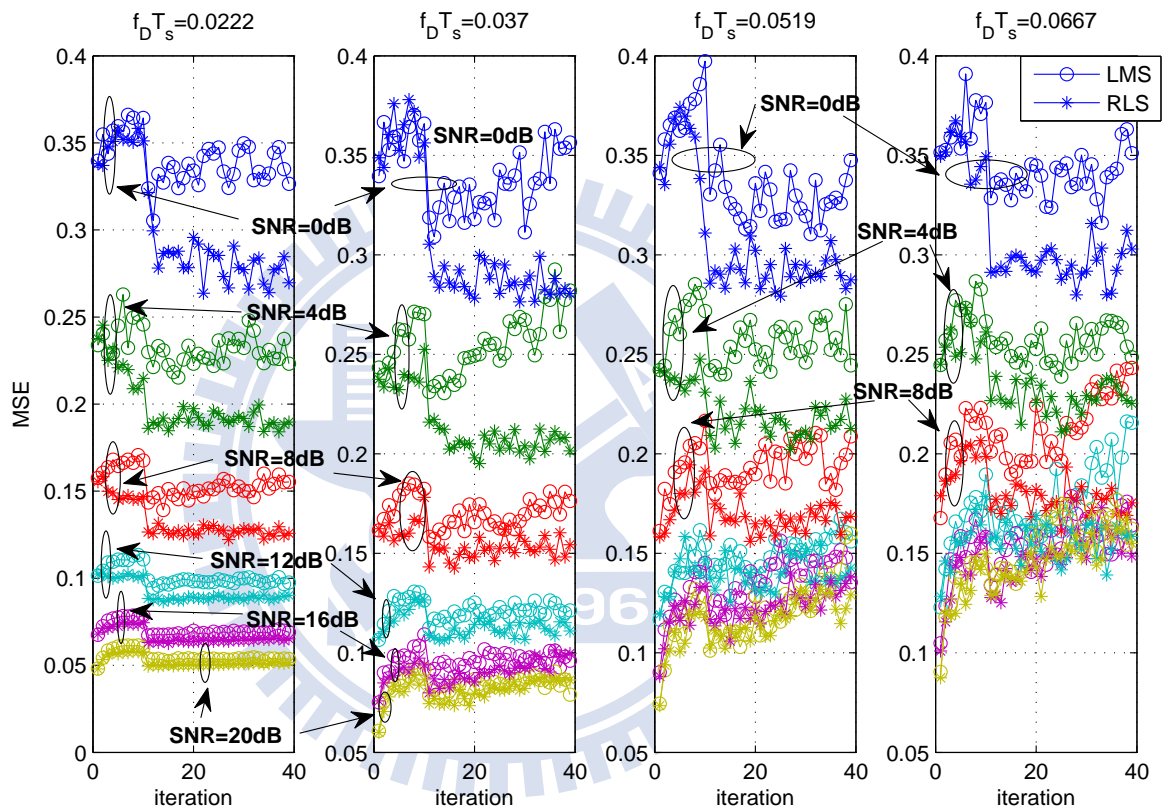


Figure 3.9: MSE of RLS and LMS 3 bits/transmission, $N = 40$.

Chapter 4

Spatio-Temporal Correlation and Channel Estimation Error-Aware ML Detection

As the so-called ML MIMO detector (2.10) maximizes likelihood and thus minimizes symbol error rate (SER) when full CSIR is available, it becomes strictly suboptimal when only partial CSI or channel estimate is available at the receiver and is alternatively referred to as the mismatched detector

$$\hat{\mathbf{X}}^{\text{MM}}(k) \stackrel{\text{def}}{=} \arg \min_{[\tilde{\mathbf{X}}]_{ij} \in \mathcal{A}_M \cup \{0\}} \|\mathbf{Y}(k) - \hat{\mathbf{H}}\tilde{\mathbf{X}}\|_F, \quad (4.1)$$

where $\hat{\mathbf{H}} = \hat{\mathbf{H}}(k)$ for MB estimators and $\hat{\mathbf{H}}(k-1)$ for DD ones. In this chapter, the real ML detectors corresponding to LS decision-directed and model-based channel estimators are derived. While most of the existing researches assume channel to be time-invariant within a frame, i.e., pilot and data transmission over the same channel, throughout this work, a more general environment is adopted. The channel varies from block to block and is spatio-temporally correlated. In the next section, the ML detector based on MB

channel estimation is given first. The following lemma is useful for deriving our proposed detectors throughout the work.

Lemma: Let \mathbf{z}_1 and \mathbf{z}_2 be circularly symmetric complex Gaussian random vectors with zero means and full-rank covariance matrices $\Sigma_{ij} \stackrel{def}{=} \mathbb{E}\{\mathbf{z}_i \mathbf{z}_j^H\}$. Then, conditioned on \mathbf{z}_2 , the random vector \mathbf{z}_1 is circularly symmetric Gaussian with mean $\Sigma_{12} \Sigma_{22}^{-1} \mathbf{z}_2$ and covariance matrix $\Sigma_{11} - \Sigma_{12} \Sigma_{22}^{-1} \Sigma_{21}$.

4.1 ML Detection With MB Channel Estimates

4.1.1 Universal MIMO Signal Detection

While the well-known Frobenius norm-based metric fails to optimize SER, the true ML detector shall be derived. Recall that with MB channel estimate $\hat{\mathbf{H}}(k)$, the *universal* ML MIMO detection shall be done with the maximization of likelihood function

$$P\left(\text{vec}(\mathbf{Y}(k)) \mid \text{vec}(\mathbf{X}(k)), \text{vec}(\hat{\mathbf{H}}(k))\right). \quad (4.2)$$

Since the entries of $\mathbf{Y}(k)$ and $\hat{\mathbf{H}}(k)$ are all zero-mean, invoking *Lemma* with

$$\begin{aligned} \mathbf{z}_1 &= \text{vec}(\mathbf{Y}(k)) = \text{vec}(\mathbf{H}(k)) \odot \text{vec}(\mathbf{X}(k)) + \text{vec}(\mathbf{Z}(k)), \\ \mathbf{z}_2 &= \text{vec}(\hat{\mathbf{H}}(k)) \\ &= \left[\text{vec}(\mathbf{Y}(k_p)) \quad \text{vec}(\mathbf{Y}(k_p + N)) \quad \text{vec}(\mathbf{Y}(k_p + 2N)) \right] \left(\mathbf{t}^H(k) \mathbf{T}^{-1}(k_p) \right)^T \end{aligned} \quad (4.3)$$

helps us obtain (4.2). Specifically, with

$$\begin{aligned} \Sigma_{11} &= \mathbb{E}\{\mathbf{z}_1 \mathbf{z}_1^H\} = (\mathbf{X}^T(k) \otimes \mathbf{I}_{N_R}) \Phi (\mathbf{X}^*(k) \otimes \mathbf{I}_{N_R}) + \sigma_z^2 \mathbf{I}_{N_R N_T}, \\ \Sigma_{12} &= \mathbb{E}\{\mathbf{z}_1 \mathbf{z}_2^H\} = \mathbf{t}^H(k) \mathbf{T}^{-1}(k_p) \mathbf{q}(k) (\mathbf{X}^T(k) \otimes \mathbf{I}_{N_R}) \Phi, \\ \Sigma_{22} &= \mathbb{E}\{\mathbf{z}_2 \mathbf{z}_2^H\} = \nu(k) \Phi + \sigma_z^2 \left\| \mathbf{t}^H(k) \mathbf{T}^{-1}(k_p) \right\|_F^2 \mathbf{I}_{N_R N_T}, \end{aligned} \quad (4.4)$$

we are able to find the conditional mean and covariance of $\mathbf{Y}(k)$ given $\mathbf{X}(k)$ and $\hat{\mathbf{H}}(k)$:

$$\boldsymbol{\Sigma}_{12}\boldsymbol{\Sigma}_{22}^{-1}\mathbf{z}_2 = (\mathbf{X}^T(k) \otimes \mathbf{I}_{N_R}) \mathbf{A}(k)\text{vec}(\hat{\mathbf{H}}(k)), \quad (4.5)$$

$$\begin{aligned} \boldsymbol{\Sigma}_{11} - \boldsymbol{\Sigma}_{12}\boldsymbol{\Sigma}_{22}^{-1}\boldsymbol{\Sigma}_{12}^H &= \sigma_z^2 \mathbf{I}_{BN_R} + (\mathbf{X}^T(k) \otimes \mathbf{I}_{N_R}) \\ &\cdot (\mathbf{I}_{N_R N_T} - \mathbf{A}(k)\mathbf{t}^H(k)\mathbf{T}^{-1}(k_p)\mathbf{q}(k)) \boldsymbol{\Phi}(\mathbf{X}^*(k) \otimes \mathbf{I}_{N_R}) \\ &\stackrel{\text{def}}{=} \mathbf{D}(k) \end{aligned} \quad (4.6)$$

where

$$\begin{aligned} \mathbf{q}(k) &= [\rho_T(k - k_p), \rho_T(k - k_p - N), \rho_T(k - k_p - 2N)]^T, \\ \boldsymbol{\nu}(k) &= \mathbf{t}^H(k)\mathbf{T}^{-1}(k_p) \begin{bmatrix} 1 & \rho_T(N) & \rho_T(2N) \\ \rho_T(N) & 1 & \rho_T(N) \\ \rho_T(2N) & \rho_T(N) & 1 \end{bmatrix} (\mathbf{t}^H(k)\mathbf{T}^{-1}(k_p))^H, \\ \mathbf{A}(k) &= \boldsymbol{\Phi} \mathbf{t}^H(k)\mathbf{T}^{-1}(k_p)\mathbf{q}(k)\boldsymbol{\Sigma}_{22}^{-1}. \end{aligned} \quad (4.7)$$

Finally, the ML detector with MB channel estimates for *universal* MIMO system is obtained:

$$\begin{aligned} \hat{\mathbf{X}}^{\text{ML}}(k) &= \arg \min_{\{\tilde{\mathbf{X}}\}_{ij} \in \mathcal{A}_M \cup \{0\}} \log \det \tilde{\mathbf{D}}(k) \\ &\quad + \left(\text{vec}(\mathbf{Y}(k)) - \left(\tilde{\mathbf{X}}^T \otimes \mathbf{I}_{N_R} \right) \mathbf{A}(k)\text{vec}(\hat{\mathbf{H}}(k)) \right)^H \tilde{\mathbf{D}}^{-1}(k) \\ &\quad \cdot \left(\text{vec}(\mathbf{Y}(k)) - \left(\tilde{\mathbf{X}}^T \otimes \mathbf{I}_{N_R} \right) \mathbf{A}(k)\text{vec}(\hat{\mathbf{H}}(k)) \right). \end{aligned} \quad (4.8)$$

Note that instead of $\mathbf{D}(k)$, $\tilde{\mathbf{D}}(k)$ is used because $\mathbf{D}(k)$ is a function of $\mathbf{X}(k)$ and thus varies with candidate blocks.

While in the above derivation no assumption has been made on the structure of data matrix $\mathbf{X}(k)$, i.e., it can carry spatial-multiplexed, spatial-modulated symbols, etc., we specifically find the ML detectors for SM systems with QAM or PSK-modulated symbols

which are of lower complexity than (4.8) due to the simplicity of SM in the following.

4.1.2 An Alternative Perspective on ML Detector Derivation

From another point of view, we can express in terms of $\hat{\mathbf{H}}$ which is estimated by Model-Based estimator as

$$\hat{\mathbf{H}}(k) = \mathbf{H}(k) + \mathbf{E}(k) \quad (4.9)$$

where $\mathbf{E}(k)$ is the channel estimation error matrix. And we can express the error matrix as follow

$$\begin{aligned} \text{vec}(\mathbf{E}(k)) &= \text{vec}(\hat{\mathbf{H}}(k)) - \text{vec}(\mathbf{H}(k)) \\ &= \left[\text{vec}(\mathbf{Y}(k_p)) \text{vec}(\mathbf{Y}(k_p + N)) \text{vec}(\mathbf{Y}(k_p + 2N)) \right] \left(\mathbf{t}^H(k) \mathbf{T}^{-1}(k_p) \right)^T - \text{vec}(\mathbf{H}(k)) \end{aligned} \quad (4.10)$$

Then, we have the mean and covariance matrix of $\mathbf{E}(k)$

$$\begin{aligned} \mathbb{E} \left\{ \text{vec}(\mathbf{E}(k)) \right\} &= \mathbf{0} \\ \mathbb{E} \left\{ \text{vec}(\mathbf{E}(k)) \text{vec}(\mathbf{E}(k))^H \right\} &= (\nu(k) - 2\mathbf{t}^H(k) \mathbf{T}^{-1}(k_p) \mathbf{q}(k) + 1) \mathbf{\Phi} + \sigma_z^2 \left\| \mathbf{t}^H(k) \mathbf{T}^{-1}(k_p) \right\|_F^2 \mathbf{I}_{N_R N_T} \end{aligned} \quad (4.11)$$

At the receiver side we have

$$\begin{aligned} \mathbf{Y}(k) &= \hat{\mathbf{H}}(k) \mathbf{X}(k) + \left(\mathbf{Z}(k) - \mathbf{E}(k) \mathbf{X}(k) \right) \\ &= \hat{\mathbf{H}}(k) \mathbf{X}(k) + \mathbf{W}(k) \end{aligned} \quad (4.12)$$

where $\mathbf{W}(k)$ is the colored noise.

To derive the ML detector, we invoke *Lemma* with $\mathbf{z}_1 = \text{vec}(\mathbf{Y}(k))$ and

$$\begin{aligned} \mathbf{z}_2 &= \text{vec}(\hat{\mathbf{H}}(k)) \\ &= \left[\text{vec}(\mathbf{Y}(k_p)) \text{vec}(\mathbf{Y}(k_p + N)) \text{vec}(\mathbf{Y}(k_p + 2N)) \right] \left(\mathbf{t}^H(k) \mathbf{T}^{-1}(k_p) \right)^T \end{aligned} \quad (4.13)$$

and with (4.11), (4.12), we can have the following parameters

$$\begin{aligned} \Sigma_{11} &= \mathbb{E}\{\mathbf{z}_1 \mathbf{z}_1^H\} = (\mathbf{X}^T(k) \otimes \mathbf{I}_{N_R}) \Phi (\mathbf{X}^*(k) \otimes \mathbf{I}_{N_R}) + \sigma_z^2 \mathbf{I}_{N_R N_T}, \\ \Sigma_{12} &= \mathbb{E}\{\mathbf{z}_1 \mathbf{z}_2^H\} = \mathbf{t}^H(k) \mathbf{T}^{-1}(k_p) \mathbf{q}(k) (\mathbf{X}^T(k) \otimes \mathbf{I}_{N_R}) \Phi, \\ \Sigma_{22} &= \mathbb{E}\{\mathbf{z}_2 \mathbf{z}_2^H\} = \nu(k) \Phi + \sigma_z^2 \|\mathbf{t}^H(k) \mathbf{T}^{-1}(k_p)\|_F^2 \mathbf{I}_{N_R N_T}, \end{aligned} \quad (4.14)$$

Finally, we have the universal ML detector.

$$\begin{aligned} \hat{\mathbf{X}}^{\text{ML}}(k) &= \arg \min_{[\tilde{\mathbf{X}}]_{ij} \in \mathcal{A}_M \cup \{0\}} \log \det \tilde{\mathbf{D}}(k) \\ &\quad + \left(\text{vec}(\mathbf{Y}(k)) - \left(\tilde{\mathbf{X}}^T \otimes \mathbf{I}_{N_R} \right) \mathbf{A}(k) \text{vec}(\hat{\mathbf{H}}(k)) \right)^H \tilde{\mathbf{D}}^{-1}(k) \\ &\quad \cdot \left(\text{vec}(\mathbf{Y}(k)) - \left(\tilde{\mathbf{X}}^T \otimes \mathbf{I}_{N_R} \right) \mathbf{A}(k) \text{vec}(\hat{\mathbf{H}}(k)) \right). \end{aligned} \quad (4.15)$$

which has exactly the same as (4.8).

4.1.3 ML Spatial-Modulated Signal Detectors

Because we may let candidate $\tilde{\mathbf{X}} = \tilde{\mathbf{L}} \tilde{\mathbf{S}}$ with $\tilde{\mathbf{S}} = \text{Diag}(\tilde{s}_1, \tilde{s}_2, \dots, \tilde{s}_B)$ and

$$[\tilde{\mathbf{L}}]_{ij} = \begin{cases} 1, & \text{if } i = \tilde{\ell}_j; \\ 0, & \text{otherwise,} \end{cases} \quad (4.16)$$

the dedicated ML detector for SM signals using different \mathcal{A}_M are derived with $\mathbf{A}(k)$ (4.7).

► ***M*-PSK**

For SM MIMO system using *M*-PSK \mathcal{A}_M , (4.8) can be reduced to

$$\begin{aligned} \hat{\mathbf{X}}^{\text{ML}}(k) = & \arg \min_{\tilde{s}_j \in \mathcal{A}_M, \tilde{\ell}_j \in \mathbb{L}} \log \det \tilde{\mathbf{D}}(k) \\ & + \left(\frac{1}{E_s} \text{vec}(\mathbf{Y}(k) \tilde{\mathbf{S}}^H) - (\tilde{\mathbf{L}}^T \otimes \mathbf{I}_{N_R}) \mathbf{A}(k) \text{vec}(\hat{\mathbf{H}}(k)) \right)^H \tilde{\mathbf{D}}^{-1}(k) \\ & \cdot \left(\frac{1}{E_s} \text{vec}(\mathbf{Y}(k) \tilde{\mathbf{S}}^H) - (\tilde{\mathbf{L}}^T \otimes \mathbf{I}_{N_R}) \mathbf{A}(k) \text{vec}(\hat{\mathbf{H}}(k)) \right) \end{aligned} \quad (4.17)$$

where $\tilde{\mathbf{D}}(k) \stackrel{\text{def}}{=} \frac{\sigma_z^2}{E_s} \mathbf{I}_{BN_R} + (\tilde{\mathbf{L}}^T \otimes \mathbf{I}_{N_R}) (\mathbf{I}_{N_R N_T} - \mathbf{A}(k) \mathbf{t}^H(k) \mathbf{T}^{-1}(k_p) \mathbf{q}(k)) \Phi(\tilde{\mathbf{L}}^* \otimes \mathbf{I}_{N_R})$ and $E_s = |s_j|^2, \forall j$.

► ***M*-QAM**

On the other hand, if \mathcal{A}_M denotes *M*-QAM, the ML decision rule becomes

$$\begin{aligned} \tilde{\mathbf{X}}^{\text{ML}}(k) = & \arg \min_{\tilde{s}_j \in \mathcal{A}_M, \tilde{\ell}_j \in \mathbb{L}} N_R \log \det \tilde{\mathbf{E}}_s + \log \det \tilde{\mathbf{D}}(k) \\ & + \left(\text{vec}(\mathbf{Y}(k) \tilde{\mathbf{S}}^H \tilde{\mathbf{E}}_s^{-1}) - (\tilde{\mathbf{L}}^T \otimes \mathbf{I}_{N_R}) \mathbf{A}(k) \text{vec}(\hat{\mathbf{H}}(k)) \right)^H \tilde{\mathbf{D}}^{-1}(k) \\ & \cdot \left(\text{vec}(\mathbf{Y}(k) \tilde{\mathbf{S}}^H \tilde{\mathbf{E}}_s^{-1}) - (\tilde{\mathbf{L}}^T \otimes \mathbf{I}_{N_R}) \mathbf{A}(k) \text{vec}(\hat{\mathbf{H}}(k)) \right) \end{aligned}$$

with $\tilde{\mathbf{D}}(k) \stackrel{\text{def}}{=} \sigma_z^2 (\tilde{\mathbf{E}}_s^{-1} \otimes \mathbf{I}_{N_R}) + (\tilde{\mathbf{L}}^T \otimes \mathbf{I}_{N_R}) (\mathbf{I} - \mathbf{A}(k) \mathbf{t}^H(k) \mathbf{T}^{-1}(k_p) \mathbf{q}(k)) \Phi(\tilde{\mathbf{L}}^* \otimes \mathbf{I}_{N_R})$ and $\tilde{\mathbf{E}}_s \stackrel{\text{def}}{=} \tilde{\mathbf{S}} \tilde{\mathbf{S}}^H$.

4.1.4 Complexity-Aware Near-ML *M*-PSK SM Detector

As SM detector (4.17) calls for the exhaustive search over all possible combination of active antenna-transmitted symbol pairs which belong to $\mathbb{L}^B \times \mathcal{A}_M^B$, the computational complexity is nontrivial. It is desirable to find a low-complexity counterpart that reduces the search dimension while keeping the performance loss to a minimum. To this end, we develop a two-step approach that detects the active antenna indices and then transmitted

symbols sequentially. Specifically, the maximization of

$$P(\mathbf{Y}(k) | \mathbf{L}(k), \hat{\mathbf{H}}(k)) = \sum_{s_1(k)} \sum_{s_2(k)} \cdots \sum_{s_B(k)} P(\mathbf{Y}(k) | \mathbf{L}(k), \mathbf{S}(k), \hat{\mathbf{H}}(k)) P(\mathbf{S}(k))$$

with respect to $\mathbf{L}(k)$ gives the following by letting $\tilde{\mathbf{s}} = [\tilde{s}_1, \dots, \tilde{s}_B]^T$:

$$\hat{\mathbf{L}}(k) = \arg \max_{\tilde{\mathbf{L}}} M^{-B} (\det E_s \tilde{\mathbf{D}}(k))^{-\frac{1}{2}} \sum_{\tilde{\mathbf{s}}} \exp \left(-\frac{1}{2} \tilde{\mathbf{m}}^H(k) \tilde{\mathbf{D}}^{-1}(k) \tilde{\mathbf{m}}(k) - \frac{1}{2E_s^2} \tilde{\mathbf{s}}^T \tilde{\mathbf{J}}(k) \tilde{\mathbf{s}}^* + \frac{1}{E_s} \Re\{\tilde{\mathbf{b}}^H(k) \tilde{\mathbf{s}}^*\} \right) \quad (4.18)$$

where $\tilde{\mathbf{D}}(k) \stackrel{\text{def}}{=} \frac{\sigma_z^2}{E_s} \mathbf{I}_{BN_R} + (\tilde{\mathbf{L}}^T \otimes \mathbf{I}_{N_R}) (\mathbf{I}_{N_R N_T} - \mathbf{A}(k) \mathbf{t}^H(k) \mathbf{T}^{-1}(k_p) \mathbf{q}(k)) \Phi(\tilde{\mathbf{L}}^* \otimes \mathbf{I}_{N_R})$, $\tilde{\mathbf{m}}(k) = (\tilde{\mathbf{L}}^T \otimes \mathbf{I}_{N_R}) \mathbf{A}(k) \text{vec}(\hat{\mathbf{H}}(k))$, and

$$\tilde{\mathbf{J}}(k) = \begin{bmatrix} \mathbf{y}_1^H(k) & & & & & & \mathbf{y}_1(k) \\ & \ddots & & & & & \vdots \\ & & \mathbf{y}_B^H(k) & & & & \mathbf{y}_B(k) \\ & & & \tilde{\mathbf{D}}^{-1}(k) & & & \\ & & & & \ddots & & \\ & & & & & & \mathbf{y}_B(k) \end{bmatrix}, \quad (4.19)$$

$$\tilde{\mathbf{b}}(k) = \begin{bmatrix} \mathbf{y}_1^H(k) \\ \vdots \\ \mathbf{y}_B^H(k) \\ \tilde{\mathbf{D}}^{-1}(k) \tilde{\mathbf{m}}(k) \end{bmatrix}. \quad (4.20)$$

Since for a specific $\tilde{\mathbf{L}}$, the following sum is dominated by one term:

$$\begin{aligned} \sum_{\tilde{\mathbf{s}}} \exp \left(-\frac{1}{2} \tilde{\mathbf{m}}^H(k) \tilde{\mathbf{D}}^{-1}(k) \tilde{\mathbf{m}}(k) - \frac{1}{2E_s^2} \tilde{\mathbf{s}}^T \tilde{\mathbf{J}}(k) \tilde{\mathbf{s}}^* + \frac{1}{E_s} \Re\{\tilde{\mathbf{b}}^H(k) \tilde{\mathbf{s}}^*\} \right) \\ \approx \exp \left(-\frac{1}{2} \tilde{\mathbf{m}}^H(k) \tilde{\mathbf{D}}^{-1}(k) \tilde{\mathbf{m}}(k) - \frac{1}{2E_s^2} \tilde{\mathbf{s}}^T(\tilde{\mathbf{L}}) \tilde{\mathbf{J}}(k) \tilde{\mathbf{s}}^*(\tilde{\mathbf{L}}) + \frac{1}{E_s} \Re\{\tilde{\mathbf{b}}^H(k) \tilde{\mathbf{s}}^*(\tilde{\mathbf{L}})\} \right) \end{aligned} \quad (4.21)$$

where a function of $\tilde{\mathbf{L}}$

$$\tilde{\mathbf{s}}(\tilde{\mathbf{L}}) \stackrel{\text{def}}{=} \mathcal{Q}_{AM} \left(E_s (\tilde{\mathbf{J}}^{-1}(k) \tilde{\mathbf{b}}(k))^* \right) \quad (4.22)$$

is obtained by differentiation with $\mathcal{Q}_{\mathcal{A}_M}(\cdot)$ demodulating the enclosed item to its nearest constellation points in \mathcal{A}_M .

Therefore, we have

$$\hat{\mathbf{L}}(k) \approx \arg \min_{\tilde{\mathbf{L}}} \frac{1}{2} \left(\log \det(E_s \tilde{\mathbf{D}}(k)) + \tilde{\mathbf{m}}^H(k) \tilde{\mathbf{D}}^{-1}(k) \tilde{\mathbf{m}}(k) + \frac{1}{E_s^2} \bar{\mathbf{s}}^T(\tilde{\mathbf{L}}) \tilde{\mathbf{J}}(k) \bar{\mathbf{s}}^*(\tilde{\mathbf{L}}) \right) - \frac{1}{E_s} \Re \left\{ \tilde{\mathbf{b}}^H(k) \bar{\mathbf{s}}^*(\tilde{\mathbf{L}}) \right\}. \quad (4.23)$$

Consequently, the transmitted symbol is decided as

$$\hat{\mathbf{s}}(k) = \bar{\mathbf{s}}(\hat{\mathbf{L}}(k)).$$

Compared to (4.17), the search dimension of detector (4.23) is effectively reduced.

4.2 ML Detection With DD Channel Estimates

On the other hand, in this section, the ML detector for SM system incorporating LS decision-directed channel estimator is derived. Invoking *Lemma* with $\mathbf{z}_1 \stackrel{def}{=} \text{vec}(\mathbf{Y}(k))$ and

$$\mathbf{z}_2 \stackrel{def}{=} \text{vec}(\hat{\mathbf{H}}(k-1)) = \text{vec}(\mathbf{Y}(k-1) \hat{\mathbf{X}}^\dagger(k-1)),$$

the maximization of

$$P\left(\text{vec}(\mathbf{Y}(k)) \mid \text{vec}(\mathbf{X}(k)), \text{vec}(\hat{\mathbf{H}}(k-1))\right) \quad (4.24)$$

mandates

$$\begin{aligned} \hat{\mathbf{X}}^{\text{ML}}(k) = & \arg \min_{[\tilde{\mathbf{X}}]_{ij} \in \mathcal{A}_M \cup \{0\}} \log \det \tilde{\mathbf{D}}(k) \\ & + \left(\text{vec}(\mathbf{Y}(k)) - \left(\tilde{\mathbf{X}}^T \otimes \mathbf{I}_{N_R} \right) \mathbf{A} \text{vec}(\hat{\mathbf{H}}(k-1)) \right)^H \tilde{\mathbf{D}}^{-1}(k) \\ & \cdot \left(\text{vec}(\mathbf{Y}(k)) - \left(\tilde{\mathbf{X}}^T \otimes \mathbf{I}_{N_R} \right) \mathbf{A} \text{vec}(\hat{\mathbf{H}}(k-1)) \right) \end{aligned} \quad (4.25)$$

because the conditional mean and covariance of $\mathbf{Y}(k)$ given $\mathbf{X}(k)$ and $\hat{\mathbf{H}}(k-1)$ are respectively

$$\begin{aligned} \Sigma_{12} \Sigma_{22}^{-1} \mathbf{z}_2 &= \left(\mathbf{X}^T(k) \otimes \mathbf{I}_{N_R} \right) \mathbf{A} \text{vec}(\hat{\mathbf{H}}(k-1)), \\ \Sigma_{11} - \Sigma_{12} \Sigma_{22}^{-1} \Sigma_{12}^H &= \sigma_z^2 \mathbf{I}_{BN_R} + \left(\mathbf{X}^T(k) \otimes \mathbf{I}_{N_R} \right) \left(\mathbf{I}_{N_R N_T} - \rho_T(1) \mathbf{A} \right) \Phi \left(\mathbf{X}^*(k) \otimes \mathbf{I}_{N_R} \right) \\ &\stackrel{\text{def}}{=} \mathbf{D}(k) \end{aligned}$$

with $\mathbf{A} \stackrel{\text{def}}{=} \rho_T(1) \Phi \left(\Phi + \sigma^2 \mathbf{I}_{N_R N_T} \right)^{-1}$.

4.2.1 ML Spatial-Modulated Signal Detectors

Similarly, let $\tilde{\mathbf{X}} = \tilde{\mathbf{L}} \tilde{\mathbf{S}}$ with $\tilde{\mathbf{S}} = \text{Diag}(\tilde{s}_1, \tilde{s}_2, \dots, \tilde{s}_B)$ and $\tilde{\mathbf{L}}$ defined as (4.16), we derive the dedicated ML detector for SM signals under DD channel estimation with $\mathbf{A} \stackrel{\text{def}}{=} \rho_T(1) \Phi \left(\Phi + \sigma^2 \mathbf{I}_{N_R N_T} \right)^{-1}$.

► *M*-PSK

For SM MIMO system using *M*-PSK \mathcal{A}_M , the detection may be done via

$$\begin{aligned} \hat{\mathbf{X}}^{\text{ML}}(k) = & \arg \min_{\tilde{s}_j \in \mathcal{A}_M, \tilde{\ell}_j \in \mathbb{L}} \log \det \tilde{\mathbf{D}}(k) \\ & + \left(\frac{1}{E_s} \text{vec}(\mathbf{Y}(k) \tilde{\mathbf{S}}^H) - \left(\tilde{\mathbf{L}}^T \otimes \mathbf{I}_{N_R} \right) \mathbf{A} \text{vec}(\hat{\mathbf{H}}(k-1)) \right)^H \tilde{\mathbf{D}}^{-1}(k) \\ & \cdot \left(\frac{1}{E_s} \text{vec}(\mathbf{Y}(k) \tilde{\mathbf{S}}^H) - \left(\tilde{\mathbf{L}}^T \otimes \mathbf{I}_{N_R} \right) \mathbf{A} \text{vec}(\hat{\mathbf{H}}(k-1)) \right) \end{aligned}$$

where $\tilde{\mathbf{D}}(k) \stackrel{def}{=} \frac{\sigma_z^2}{\tilde{E}_s} \mathbf{I}_{BN_R} + (\tilde{\mathbf{L}}^T \otimes \mathbf{I}_{N_R}) (\mathbf{I}_{N_R N_T} - \rho_T(1) \mathbf{A}) \Phi(\tilde{\mathbf{L}}^* \otimes \mathbf{I}_{N_R})$.

► M -QAM

As for M -QAM \mathcal{A}_M , (4.25) can be reduced to

$$\begin{aligned} \tilde{\mathbf{X}}^{\text{ML}}(k) = \arg \min_{\tilde{s}_j \in \mathcal{A}_M, \tilde{\ell}_j \in \mathbb{L}} & N_R \log \det \tilde{\mathbf{E}}_s + \log \det \tilde{\mathbf{D}}(k) \\ & + \left(\text{vec}(\mathbf{Y}(k) \tilde{\mathbf{S}}^H \tilde{\mathbf{E}}_s^{-1}) - (\tilde{\mathbf{L}}^T \otimes \mathbf{I}_{N_R}) \mathbf{A}(k) \text{vec}(\hat{\mathbf{H}}(k)) \right)^H \mathbf{D}^{-1}(k) \\ & \cdot \left(\text{vec}(\mathbf{Y}(k) \tilde{\mathbf{S}}^H \tilde{\mathbf{E}}_s^{-1}) - (\tilde{\mathbf{L}}^T \otimes \mathbf{I}_{N_R}) \mathbf{A}(k) \text{vec}(\hat{\mathbf{H}}(k)) \right) \end{aligned}$$

where $\tilde{\mathbf{D}}(k) \stackrel{def}{=} \sigma_z^2 (\tilde{\mathbf{E}}_s^{-1} \otimes \mathbf{I}_{N_R}) + (\tilde{\mathbf{L}}^T \otimes \mathbf{I}_{N_R}) (\mathbf{I} - \mathbf{A}(k) \mathbf{t}^H(k) \mathbf{T}^{-1}(k_p) \mathbf{q}(k)) \Phi(\tilde{\mathbf{L}}^* \otimes \mathbf{I}_{N_R})$.

4.2.2 Complexity-Aware Near-ML M -PSK SM Detector

Similarly, reducing the search range of (4.26) from $\mathbb{L}^B \times \mathcal{A}_M^B$ to \mathbb{L}^B is desirable and can effectively saves computational complexity. While in this subsection we also propose a low-complexity two-step approach which sequentially detects the antenna indices and transmitted symbols, an alternative perspective is considered to put forward this detector. Specifically, this time, we first consider maximizing the original likelihood

$$P(\mathbf{Y}(k) | \mathbf{X}(k), \hat{\mathbf{H}}(k-1))$$

with respect to $\mathbf{X}(k)$. Then, the following is obtainable:

$$\begin{aligned}
& \max_{\tilde{\mathbf{L}}, \tilde{\mathbf{s}}} M^{-B} (\det E_s \tilde{\mathbf{D}}(k))^{-\frac{1}{2}} \exp \left(-\frac{1}{2} \tilde{\mathbf{m}}^H(k) \tilde{\mathbf{D}}^{-1}(k) \tilde{\mathbf{m}}(k) - \frac{1}{2E_s^2} \tilde{\mathbf{s}}^T \tilde{\mathbf{J}}(k) \tilde{\mathbf{s}}^* \right. \\
& \qquad \qquad \qquad \left. + \frac{1}{E_s} \Re \{ \tilde{\mathbf{b}}^H(k) \tilde{\mathbf{s}}^* \} \right) \\
& \approx \max_{\tilde{\mathbf{L}}} (\det E_s \tilde{\mathbf{D}}(k))^{-\frac{1}{2}} \exp \left(-\frac{1}{2} \tilde{\mathbf{m}}^H(k) \tilde{\mathbf{D}}^{-1}(k) \tilde{\mathbf{m}}(k) \right) \\
& \qquad \qquad \qquad \cdot \max_{\tilde{\mathbf{s}}} \exp \left(-\frac{1}{2E_s^2} \tilde{\mathbf{s}}^T \tilde{\mathbf{J}}(k) \tilde{\mathbf{s}}^* + \frac{1}{E_s} \Re \{ \tilde{\mathbf{b}}^H(k) \tilde{\mathbf{s}}^* \} \right) \\
& = \max_{\tilde{\mathbf{L}}} (\det E_s \tilde{\mathbf{D}}(k))^{-\frac{1}{2}} \exp \left(-\frac{1}{2} \tilde{\mathbf{m}}^H(k) \tilde{\mathbf{D}}^{-1}(k) \tilde{\mathbf{m}}(k) - \frac{1}{2E_s^2} \tilde{\mathbf{s}}^T(\tilde{\mathbf{L}}) \tilde{\mathbf{J}}(k) \tilde{\mathbf{s}}^*(\tilde{\mathbf{L}}) \right. \\
& \qquad \qquad \qquad \left. + \frac{1}{E_s} \Re \{ \tilde{\mathbf{b}}^H(k) \tilde{\mathbf{s}}^*(\tilde{\mathbf{L}}) \} \right)
\end{aligned} \tag{4.26}$$

where $\tilde{\mathbf{J}}(k)$, $\tilde{\mathbf{b}}(k)$, and $\tilde{\mathbf{s}}(\tilde{\mathbf{L}})$ are defined respectively as (4.19), (4.20), and (4.22) and $\tilde{\mathbf{m}}(k) = (\tilde{\mathbf{L}}^T \otimes \mathbf{I}_{N_R}) \text{Avec}(\hat{\mathbf{H}}(k-1))$ and $\tilde{\mathbf{D}}(k) = \frac{\sigma_z^2}{E_s} \mathbf{I}_{BN_R} + (\tilde{\mathbf{L}}^T \otimes \mathbf{I}_{N_R}) (\mathbf{I}_{N_R N_T} - \rho_T(1) \mathbf{A}) \Phi(\tilde{\mathbf{L}}^* \otimes \mathbf{I}_{N_R})$.

As a result, a two-step detection which has the same structure as (4.23) is obtained:

$$\begin{aligned}
\hat{\mathbf{L}}(k) &= \arg \min_{\tilde{\mathbf{L}}} \frac{1}{2} \left(\log \det(E_s \tilde{\mathbf{D}}(k)) + \tilde{\mathbf{m}}^H(k) \tilde{\mathbf{D}}^{-1}(k) \tilde{\mathbf{m}}(k) + \frac{1}{E_s^2} \tilde{\mathbf{s}}^T(\tilde{\mathbf{L}}) \tilde{\mathbf{J}}(k) \tilde{\mathbf{s}}^*(\tilde{\mathbf{L}}) \right. \\
& \qquad \qquad \qquad \left. - \frac{1}{E_s} \Re \{ \tilde{\mathbf{b}}^H(k) \tilde{\mathbf{s}}^*(\tilde{\mathbf{L}}) \} \right), \\
\hat{\mathbf{s}}(k) &= \tilde{\mathbf{s}}(\hat{\mathbf{L}}(k)).
\end{aligned}$$

4.3 Simulation Results

In this section we first compare the bit error rate (BER) performance of the derived ML MIMO signal detector and that of the mismatched detectors, and then compare the performance of the derived approximated ML SM signal detector and ML SM signal detector.

In the first comparison, we operating the detector in spatial-time correlated channel

being estimated by the model-based method. And we adopted the system model described in Section 2.1 with $B = N_T = N_R = 2$ and the rest of the environment setting are the same as in Section 5.3.

In Fig.4.1-4.3, we show the BER comparison of mismatched detector and proposed ML detector both using model-based channel estimation with different values of antenna spacing and of velocity in conventional MIMO systems. The frame size and the data rate are 10 and 4 bits/transmission respectively with QPSK modulation being used. We can see that as the antenna spacing goes small which means more correlated channel, the BER goes large as expected, and the performance improvement with respect to the mismatched detector goes large. A high modulation order is shown in Fig.4.4-4.5.

Fig.4.6-4.7 show the BER comparison of mismatched detector and proposed ML detector with DD channel estimator. Both figures show that the proposed ML detector outperform the mismatched detector, and the ML detector with DD channel estimator is more robust to channel aging than it with MB channel estimator.

Fig.4.8 and Fig.4.9 show the performance comparison of the complexity-reduced detector (4.23) and the proposed ML detector (4.17). We see that the performance these two detector are very similar to each other which is independent of spatial correlation and velocity. These two figures show that the two dimension maximization problem can be reduced into one dimension problem with nearly no performance degradation.

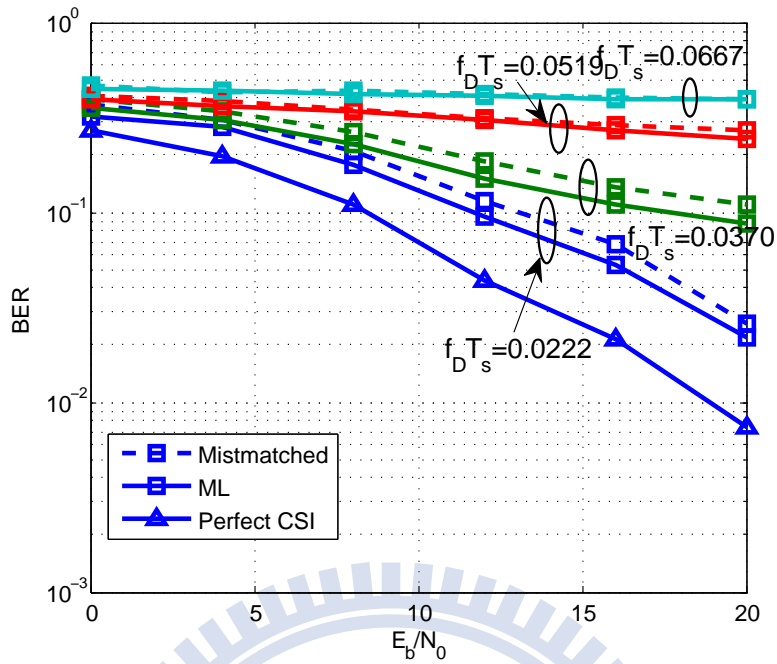


Figure 4.1: Performance of the various detectors with model-based channel estimate in time- and spatial- correlated channel; $\xi = 0.1\lambda$, 4 bits/transmission, $N = 10$ in 2×2 MIMO system.

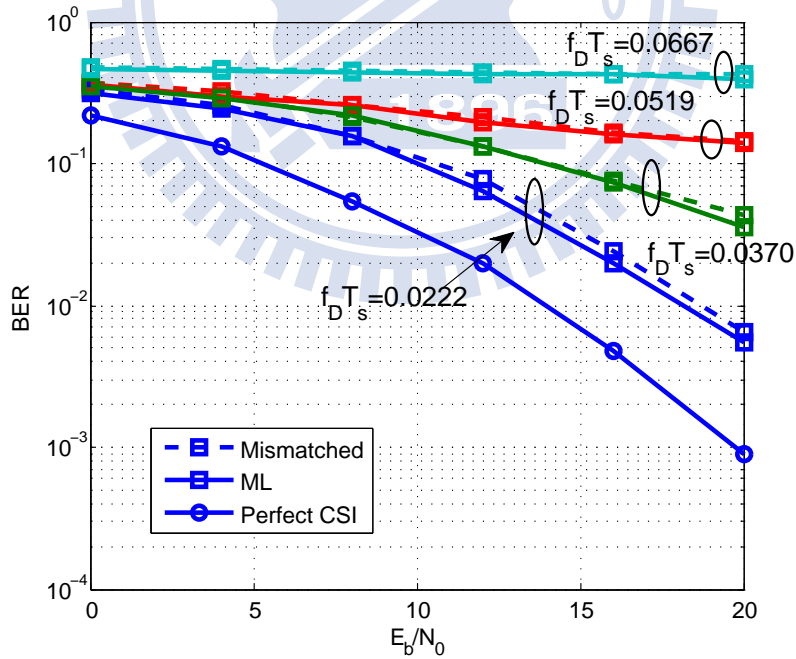


Figure 4.2: Performance of the various detectors with model-based channel estimate in time- and spatial- correlated channel; $\xi = 1\lambda$, 4 bits/transmission, $N = 10$ in 2×2 MIMO system.

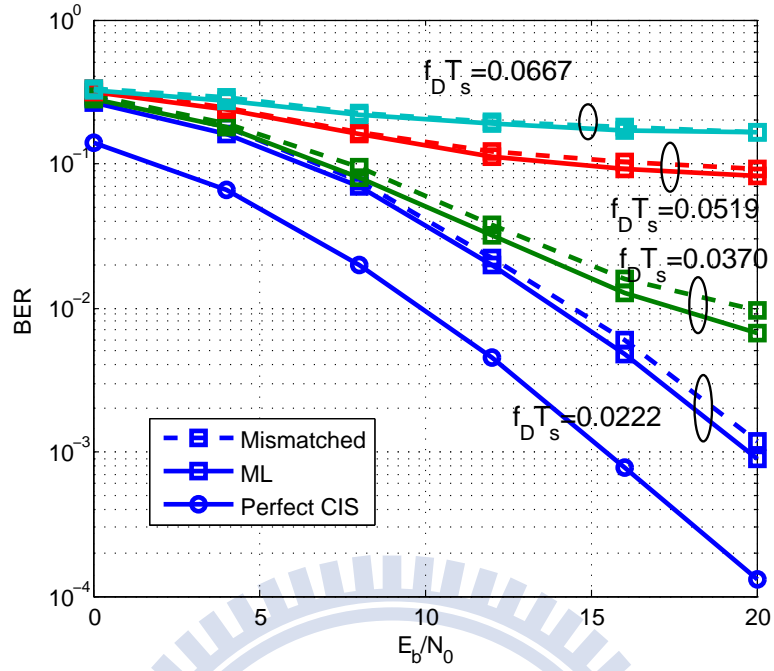


Figure 4.3: Performance of the various detectors with model-based channel estimate in time- and spatial- correlated channel; $\xi = 5\lambda$, 4 bits/transmission, $N = 10$ in 2×2 MIMO system.

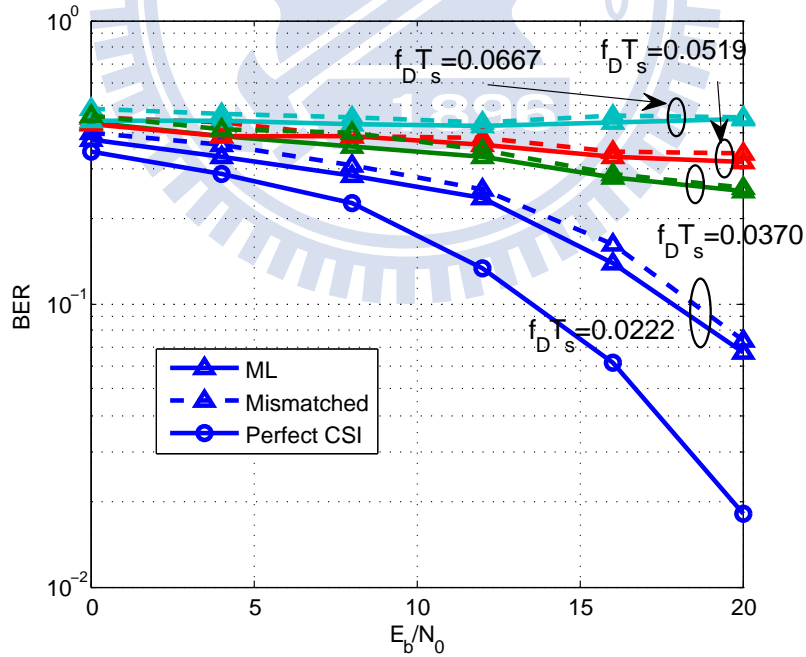


Figure 4.4: Performance of the various detectors with model-based channel estimate in time- and spatial- correlated channel; $\xi = 1\lambda$, 8 bits/transmission, $N = 10$ in 2×2 MIMO system.

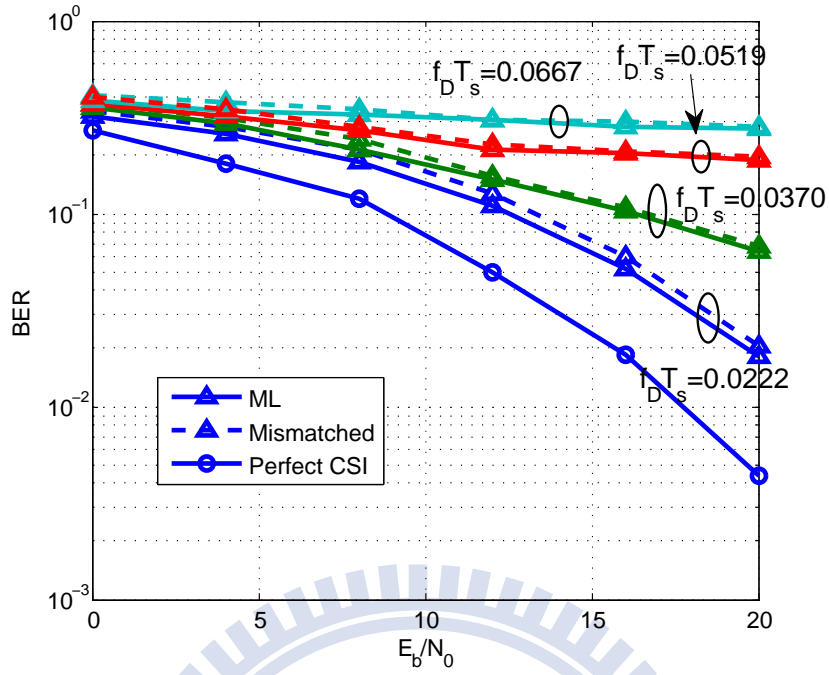


Figure 4.5: Performance of the various detectors with model-based channel estimate in time- and spatial- correlated channel; $\xi = 5\lambda$, 8 bits/transmission, $N = 10$ in 2×2 MIMO system.

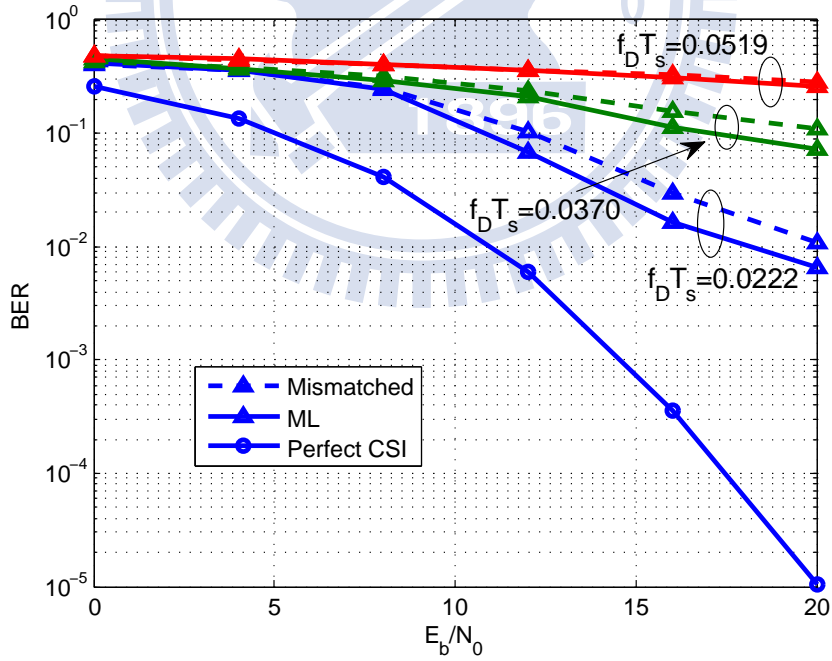


Figure 4.6: Performance of the various detectors with decision-directed channel estimate in time- and spatial- correlated channel; $\xi = 1\lambda$, 4 bits/transmission, $N = 10$ in 4×4 MIMO system.

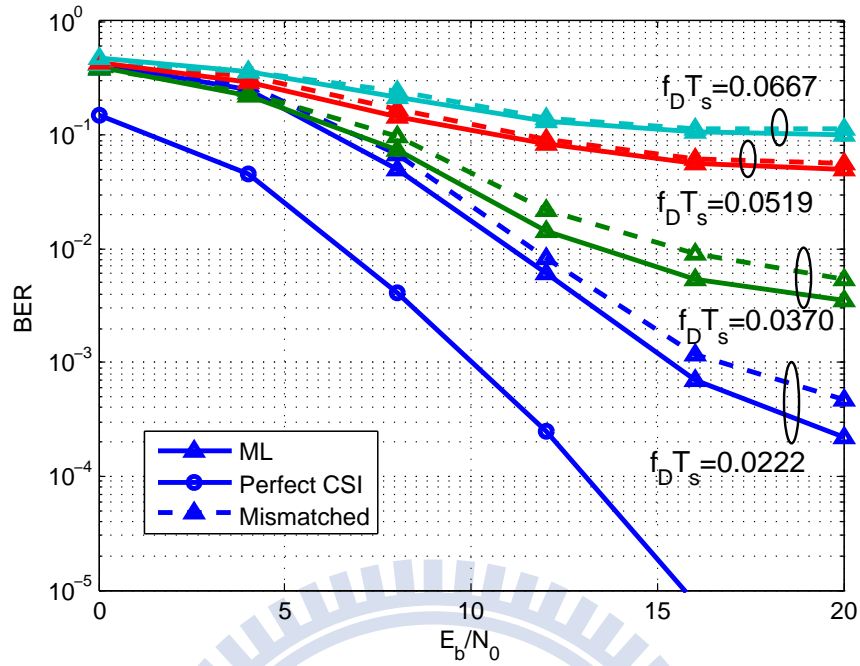


Figure 4.7: Performance of the various detectors with decision-directed channel estimate in time- and spatial- correlated channel; $\xi = 5\lambda$, 4 bits/transmission, $N = 10$ in 4×4 MIMO system.

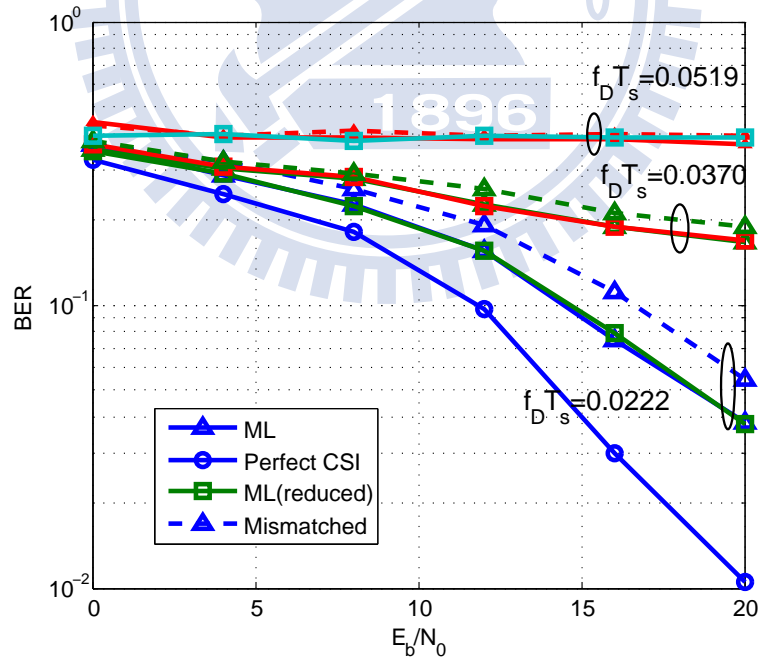


Figure 4.8: Performance of the various detectors with model-based channel estimate in time- and spatial- correlated channel; $\xi = 0.1\lambda$, 4 bits/transmission, $N = 10$ in 4×4 SM MIMO system.

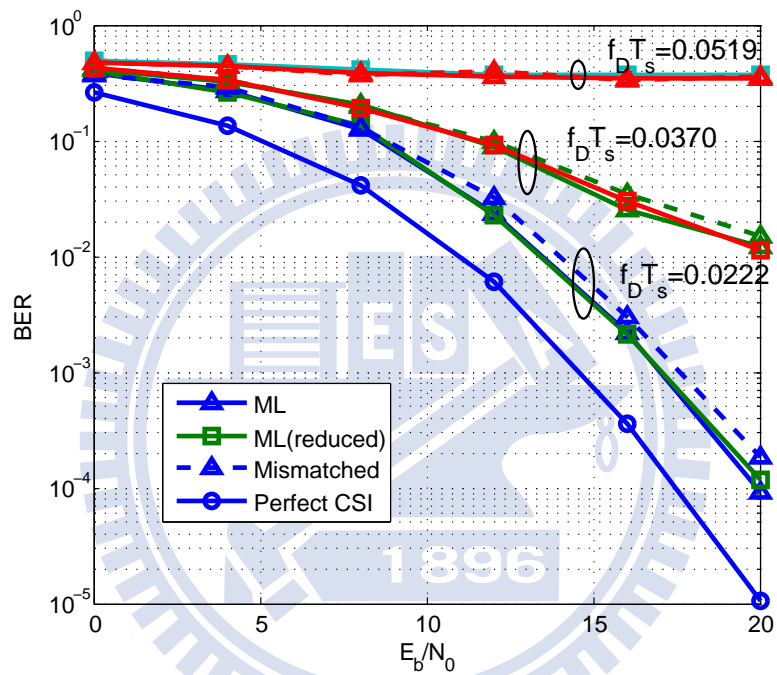


Figure 4.9: Performance of the various detectors with model-based channel estimate in time- and spatial- correlated channel; $\xi = 1\lambda$, 4 bits/transmission, $N = 10$ in 4×4 SM MIMO system.

Chapter 5

Approximated Maximum-Likelihood MIMO Detection

Unlike in Section 4.1.4 and 4.2.2, only PSK SM signal constellations are considered, in this chapter we aim to reduce the detection complexity of ML criterion for all sorts of MIMO systems.

5.1 Approximated ML Detection With MB Channel Estimates

5.1.1 Universal MIMO Signal Detection

Originated from the fact that

$$P(\mathbf{Y}(k)|\mathbf{X}(k), \hat{\mathbf{H}}(k)) \approx \prod_{r=1}^{N_R} P(\mathbf{Y}_r(k)|\mathbf{X}(k), \hat{\mathbf{H}}_r(k)), \quad (5.1)$$

matrix computation effort can be relieved due to this matrix-to-vector transformation.

By letting

$$\begin{aligned}\mathbf{z}_1^H &\stackrel{def}{=} \mathbf{Y}_r(k) = \mathbf{H}_r(k)\mathbf{X}(k) + \mathbf{Z}_r(k), \\ \mathbf{z}_2^H &\stackrel{def}{=} \hat{\mathbf{H}}_r(k) = \mathbf{t}^H(k)\mathbf{T}^{-1}(k_p) \left[\tilde{\mathbf{y}}_{r,1}, \tilde{\mathbf{y}}_{r,2}, \dots, \tilde{\mathbf{y}}_{r,N_T} \right],\end{aligned}$$

based on the *Lemma* we have the conditional mean and covariance of $\mathbf{Y}_r(k)$ given $\mathbf{X}(k)$ and $\hat{\mathbf{H}}_r(k)$ respectively as

$$\mathbf{z}_2^H \boldsymbol{\Sigma}_{22}^{-1} \boldsymbol{\Sigma}_{12}^H = \hat{\mathbf{H}}_r(k) \mathbf{A}(k) \mathbf{X}(k) \quad (5.2)$$

$$\begin{aligned}\boldsymbol{\Sigma}_{11} - \boldsymbol{\Sigma}_{12} \boldsymbol{\Sigma}_{22}^{-1} \boldsymbol{\Sigma}_{12}^H &= \sigma_z^2 \mathbf{I}_B + \mathbf{X}^H(k) (\mathbf{I} - \mathbf{A}(k) \mathbf{t}^H(k) \mathbf{T}^{-1}(k_p) \mathbf{q}(k)) \boldsymbol{\Phi}_T \mathbf{X}(k) \\ &\stackrel{def}{=} \mathbf{D}(k),\end{aligned} \quad (5.3)$$

where

$$\begin{aligned}\boldsymbol{\Sigma}_{11} &= \mathbf{X}^H(k) \boldsymbol{\Phi}_T \mathbf{X}(k) + \sigma_z^2 \mathbf{I}_B; \\ \boldsymbol{\Sigma}_{12} &= \mathbf{t}^H(k) \mathbf{T}^{-1}(k_p) \mathbf{q}(k) \mathbf{X}^H(k) \boldsymbol{\Phi}_T; \\ \boldsymbol{\Sigma}_{22} &= \nu(k) \boldsymbol{\Phi}_T + \sigma_z^2 \|\mathbf{t}^H(k) \mathbf{T}^{-1}(k_p)\|_F^2 \mathbf{I}_{N_T},\end{aligned} \quad (5.4)$$

with $\mathbf{A}(k) \stackrel{def}{=} \boldsymbol{\Phi}_T \mathbf{t}^H(k) \mathbf{T}^{-1}(k_p) \mathbf{q}(k) \boldsymbol{\Sigma}_{22}^{-1}$, $[\boldsymbol{\Phi}_T]_{ij} = \rho_S(0, j-i)$, $\mathbf{q}(k) = \left[\rho_T(k-k_p), \rho_T(k-k_p-N), \rho_T(k-k_p-2N) \right]^T$, and

$$\nu(k) = \mathbf{t}^H(k) \mathbf{T}^{-1}(k_p) \begin{bmatrix} 1 & \rho_T(N) & \rho_T(2N) \\ \rho_T(N) & 1 & \rho_T(N) \\ \rho_T(2N) & \rho_T(N) & 1 \end{bmatrix} \left(\mathbf{t}^H(k) \mathbf{T}^{-1}(k_p) \right)^H. \quad (5.5)$$

As a result, maximizing (5.1), gives an approximated ML (AML) detector:

$$\hat{\mathbf{X}}(k) = \arg \min_{[\tilde{\mathbf{X}}]_{ij} \in \mathcal{A}_M \cup \{0\}} N_R \log \det \mathbf{D}(k) + \text{tr} \left\{ \left(\mathbf{Y}(k) - \hat{\mathbf{H}}(k) \mathbf{A}(k) \tilde{\mathbf{X}} \right) \tilde{\mathbf{D}}^{-1}(k) \cdot \left(\mathbf{Y}(k) - \hat{\mathbf{H}}(k) \mathbf{A}(k) \tilde{\mathbf{X}} \right)^H \right\}. \quad (5.6)$$

Note that the approximation made in (5.1) becomes exact when channel is spatially-uncorrelated [28], i.e., $\Phi = \mathbf{I}_{N_R N_T}$.

5.1.2 Complexity-Aware AML M -PSK SM Detector

Similarly, for SM system carrying M -PSK symbols drawn from \mathcal{A}_M , AML detector (5.6) can be simplified to

$$\hat{\mathbf{X}}(k) = \arg \min_{\tilde{s}_j \in \mathcal{A}_M, \tilde{\ell}_j \in \mathbb{L}} N_R \log \det(E_s \tilde{\mathbf{D}}(k)) + \text{tr} \left\{ \left(\frac{1}{E_s} \mathbf{Y}(k) \tilde{\mathbf{S}}^H - \hat{\mathbf{H}}(k) \mathbf{A}(k) \tilde{\mathbf{L}} \right) \tilde{\mathbf{D}}^{-1}(k) \cdot \left(\frac{1}{E_s} \mathbf{Y}(k) \tilde{\mathbf{S}}^H - \hat{\mathbf{H}}(k) \mathbf{A}(k) \tilde{\mathbf{L}} \right)^H \right\} \quad (5.7)$$

where $\tilde{\mathbf{D}}(k) \stackrel{\text{def}}{=} \frac{\sigma_z^2}{E_s} \mathbf{I}_B + \tilde{\mathbf{L}}^H (\mathbf{I}_{N_T} - \mathbf{A}(k) \mathbf{t}^H(k) \mathbf{T}^{-1}(k_p) \mathbf{q}(k)) \Phi_T \tilde{\mathbf{L}}$. In addition, the two-step approach that detects the active transmit antenna indices first can also be done to further reduce the detection complexity of the AML detector (5.7). Specifically, the complexity-reduced AML is given as

$$\hat{\mathbf{L}}(k) = \arg \min_{\tilde{\mathbf{L}}} N_R \log \det(E_s \tilde{\mathbf{D}}(k)) + \text{tr} \left(\tilde{\mathbf{M}}(k) \tilde{\mathbf{D}}^{-1}(k) \tilde{\mathbf{M}}^H(k) \right) + \frac{1}{E_s^2} \bar{\mathbf{s}}^H(\tilde{\mathbf{L}}) \tilde{\mathbf{J}}(k) \bar{\mathbf{s}}(\tilde{\mathbf{L}}) - \frac{2}{E_s} \Re \{ \tilde{\mathbf{b}}^T(k) \bar{\mathbf{s}}(\tilde{\mathbf{L}}) \} \quad (5.8)$$

and $\hat{\mathbf{s}}(k) = \bar{\mathbf{s}}(\hat{\mathbf{L}}(k))$ where $\tilde{\mathbf{M}}(k) = \hat{\mathbf{H}}(k) \mathbf{A}(k) \tilde{\mathbf{L}}$, $\tilde{\mathbf{J}}(k) = \tilde{\mathbf{D}}^{-1}(k) \odot (\mathbf{Y}^H(k) \mathbf{Y}(k))^*$, $\tilde{\mathbf{b}}(k)$ equals to the diagonal of $\mathbf{Y}^H(k) \tilde{\mathbf{M}}(k) \tilde{\mathbf{D}}^{-1}(k)$, and $\bar{\mathbf{s}}(\tilde{\mathbf{L}}) = \mathcal{Q}_{\mathcal{A}_M} \left(E_s (\tilde{\mathbf{b}}^T(k) \tilde{\mathbf{J}}^{-1}(k))^H \right)$.

5.1.3 Estimation of Channel Correlation

While the successfulness of the exact and approximated ML detection in a correlated environment relies on the perfect knowledge of channel correlation, in real world applications just like the channel itself, its correlation values are also required to be estimated. Recall that $\Phi = \mathbb{E} \{ \text{vec}(\mathbf{H}(k)) \text{vec}^H(\mathbf{H}(k)) \}$, $\text{tr}(\Phi_T)\Phi_T = \mathbb{E}\{\mathbf{H}^H(k)\mathbf{H}(k)\}$, $\rho_T(k - \ell) = \mathbb{E}\{h_{ij}(k)h_{ij}^*(\ell)\}$. They may be approximated by the sample averages of the MB channel estimates $\hat{\mathbf{H}}$. Specifically,

$$\hat{\Phi}_T = \frac{1}{2N} \sum_{k=1}^{2N} \hat{\mathbf{H}}(k)^H \hat{\mathbf{H}}(k) \quad (5.9)$$

5.2 Approximated ML Detection With DD Channel Estimates

5.2.1 AML Spatial-Modulated Signal Detectors

Following the justification given in Section 4.2 and 5.1, we can also devise the approximated ML detector with partial CSI obtained by decision-directed channel estimation. Recall that the data block k is detected with the channel estimates of the previous block $\hat{\mathbf{H}}(k - 1)$. Therefore, the likelihood function aimed to be maximized becomes

$$P(\mathbf{Y}(k)|\mathbf{X}(k), \hat{\mathbf{H}}(k - 1)) \approx \prod_{r=1}^{N_R} P(\mathbf{Y}_r(k)|\mathbf{X}(k), \hat{\mathbf{H}}_r(k - 1)). \quad (5.10)$$

Invoking the *Lemma* with $\mathbf{z}_1^H = \mathbf{Y}_r(k)$ and

$$\mathbf{z}_2^H \stackrel{\text{def}}{=} \hat{\mathbf{H}}_r(k - 1) = \mathbf{H}_r(k - 1)\mathbf{G}_1(k - 1) + \mathbf{Z}_r(k - 1)\mathbf{G}_2(k - 1),$$

where $\mathbf{G}_1(k) \stackrel{def}{=} \mathbf{X}(k)\hat{\mathbf{X}}^\dagger(k)$ and $\mathbf{G}_2(k) \stackrel{def}{=} \mathbf{X}^\dagger(k)\mathbf{G}_1(k)$, we have

$$\begin{aligned}\Sigma_{11} &= \mathbf{X}^H(k)\Phi_T\mathbf{X}(k) + \sigma_z^2\mathbf{I}_B, \\ \Sigma_{12} &= \rho_T(1)\mathbf{X}^H(k)\Phi_T\mathbf{G}_1(k-1), \\ \Sigma_{22} &= \mathbf{G}_1^H(k-1)(\Phi_T + \sigma_z^2(\mathbf{X}(k-1)\mathbf{X}^H(k-1))^{-1})\mathbf{G}_1(k-1) \\ &\approx \mathbf{G}_1^H(k-1)(\Phi_T + \sigma_z^2\mathbf{I}_B)\mathbf{G}_1(k-1),\end{aligned}$$

where approximation $\mathbf{X}(k)\mathbf{X}^H(k) \approx \mathbb{E}\{\mathbf{X}(k)\mathbf{X}^H(k)\} = \mathbf{I}_{N_T}$ is applied in the last line.

Thus, given $\mathbf{X}(k)$ and $\hat{\mathbf{H}}_r(k-1)$, $\mathbf{Y}_r(k)$ has mean and covariance respectively

$$\begin{aligned}\mathbf{z}_2^H \Sigma_{22}^{-1} \Sigma_{12}^H &= \rho_T(1)\hat{\mathbf{H}}_r(k-1)(\Phi_T + \sigma_z^2\mathbf{I})^{-1}\Phi_T\mathbf{X}(k) \\ \Sigma_{11} - \Sigma_{12}\Sigma_{22}^{-1}\Sigma_{12}^H &= \sigma_z^2\mathbf{I}_B + \mathbf{X}^H(k)\left(\mathbf{I} - \rho_T(1)^2\Phi_T(\Phi_T + \sigma_z^2\mathbf{I})^{-1}\right)\Phi_T\mathbf{X}(k) \\ &\stackrel{def}{=} \mathbf{C}(k).\end{aligned}$$

The AML detector is then given by

$$\begin{aligned}\hat{\mathbf{X}}(k) &= \arg \min_{[\tilde{\mathbf{X}}]_{ij} \in \mathcal{A}_M \cup \{0\}} N_R \log \det \tilde{\mathbf{C}}(k) \\ &\quad + \text{tr} \left\{ \left(\mathbf{Y}(k) - \rho_T(1)\hat{\mathbf{H}}(k-1)(\Phi_T + \sigma_z^2\mathbf{I}_{N_T})^{-1}\Phi_T\tilde{\mathbf{X}} \right) \tilde{\mathbf{C}}^{-1}(k) \right. \\ &\quad \left. \cdot \left(\mathbf{Y}(k) - \rho_T(1)\hat{\mathbf{H}}(k-1)(\Phi_T + \sigma_z^2\mathbf{I}_{N_T})^{-1}\Phi_T\tilde{\mathbf{X}} \right)^H \right\}. \quad (5.11)\end{aligned}$$

Similarly, the approximation (5.10) becomes exact when $\Phi_T = \mathbf{I}_{N_T}$ and thus

$$\begin{aligned}\hat{\mathbf{X}}(k) &= \arg \min_{[\tilde{\mathbf{X}}]_{ij} \in \mathcal{A}_M \cup \{0\}} \sigma_z^2 N_R \log \det \tilde{\mathbf{C}}(k) + \text{tr} \left\{ \left(\mathbf{Y}(k) - \frac{\rho_T(1)}{1 + \sigma_z^2} \hat{\mathbf{H}}(k-1) \tilde{\mathbf{X}} \right) \tilde{\mathbf{C}}^{-1}(k) \right. \\ &\quad \left. \cdot \left(\mathbf{Y}(k) - \frac{\rho_T(1)}{1 + \sigma_z^2} \hat{\mathbf{H}}(k-1) \tilde{\mathbf{X}} \right)^H \right\} \quad (5.12)\end{aligned}$$

where $\mathbf{C}(k) \stackrel{def}{=} \left(\mathbf{I}_B + \left(\frac{1 + \sigma_z^2 - \rho_T^2(1)}{1 + \sigma_z^2} \right) \mathbf{X}^H(k)\mathbf{X}(k) \right)$.

5.2.2 Complexity-Aware AML M -PSK SM Detector

First, for SM system with PSK \mathcal{A}_M , the detector can be simplified as

$$\hat{\mathbf{X}}(k) = \arg \min_{\tilde{s}_j \in \mathcal{A}_M, \tilde{\ell}_j \in \mathbb{L}} N_R \log \det(E_s \tilde{\mathbf{C}}(k)) \\ + \text{tr} \left\{ \left(\frac{\mathbf{Y}(k) \tilde{\mathbf{S}}^H}{E_s} - \rho_T(1) \hat{\mathbf{H}}(k-1) (\Phi_T + \sigma_z^2 \mathbf{I}_{N_T})^{-1} \Phi_T \tilde{\mathbf{L}} \right) \tilde{\mathbf{C}}^{-1}(k) \right. \\ \left. \cdot \left(\frac{\mathbf{Y}(k) \tilde{\mathbf{S}}^H}{E_s} - \rho_T(1) \hat{\mathbf{H}}(k-1) (\Phi_T + \sigma_z^2 \mathbf{I}_{N_T})^{-1} \Phi_T \tilde{\mathbf{L}} \right)^H \right\}$$

where $\tilde{\mathbf{C}}(k) \stackrel{\text{def}}{=} \frac{\sigma_z^2}{E_s} \mathbf{I}_B + \tilde{\mathbf{L}}^H \left(\mathbf{I}_{N_T} - \rho_T(1)^2 \Phi_T (\Phi_T + \sigma_z^2 \mathbf{I}_{N_T})^{-1} \right) \Phi_T \tilde{\mathbf{L}}$. Again, with $\mathbf{X}(k) = \mathbf{L}(k) \mathbf{S}(k)$ and DD channel estimates, the two-step complexity-reduced AML detector for SM with PSK \mathcal{A}_M mandates

$$\hat{\mathbf{L}}(k) = \arg \min_{\tilde{\mathbf{L}}} N_R \log \det(E_s \tilde{\mathbf{C}}(k)) + \text{tr} \{ \tilde{\mathbf{M}}(k) \tilde{\mathbf{C}}^{-1}(k) \tilde{\mathbf{M}}^H(k) \} \\ + \frac{1}{E_s^2} \bar{\mathbf{s}}^H(\tilde{\mathbf{L}}) \tilde{\mathbf{J}}(k) \bar{\mathbf{s}}(\tilde{\mathbf{L}}) - \frac{2}{E_s} \Re \{ \tilde{\mathbf{b}}^T(k) \bar{\mathbf{s}}(\tilde{\mathbf{L}}) \} \quad (5.13)$$

and

$$\hat{\mathbf{s}}(k) = \bar{\mathbf{s}}(\hat{\mathbf{L}}(k))$$

where $\tilde{\mathbf{M}}(k) = \rho_T(1) \hat{\mathbf{H}}(k-1) (\Phi_T + \sigma_z^2 \mathbf{I}_{N_T})^{-1} \Phi_T \tilde{\mathbf{L}}$, $\tilde{\mathbf{J}}(k) = \tilde{\mathbf{C}}^{-1}(k) \odot (\mathbf{Y}^H(k) \mathbf{Y}(k))^*$, $\tilde{\mathbf{b}}(k)$ equals to the diagonal of $\mathbf{Y}^H(k) \tilde{\mathbf{M}}(k) \tilde{\mathbf{C}}^{-1}(k)$, and $\bar{\mathbf{s}}(\tilde{\mathbf{L}}) = \mathcal{Q}_{\mathcal{A}_M} \left(E_s (\tilde{\mathbf{b}}^T(k) \tilde{\mathbf{J}}^{-1}(k))^H \right)$.

5.3 Simulation Results

In this section, we compare the BER performance of the derived Approximated ML (AML) SM signal detectors and that of the mismatched detectors. We are interested in operating these detectors in two scenarios: i) time-correlated channel with decision-

directed channel estimation; ii) channel with time-spatial correlation being estimated by the decision-directed method and model-based method. Throughout the simulation in this section, we adopt the system model described in Section 2.3 with $B = N_T = N_R = 4$ and equispaced transmit and receive antennas and choose the time-spatial correlation to follow [29] with carrier frequency $f_c = 2$ GHz and symbol time $T_s = 0.1$ ms. Specifically,

$$\rho_T(k - \ell) = J_0(2\pi f_D |k - \ell| B T_s) \quad (5.14)$$

$$\rho_S(i - m, j - n) = J_0(2\pi |(i - m)| \xi / \lambda) J_0(2\pi |(j - n)| \xi / \lambda), \quad (5.15)$$

where f_D is the maximum Doppler frequency, ξ the antenna spacing, λ the wavelength, and $J_0(\cdot)$ the zeroth-order Bessel function of the first kind. The frame structure is as depicted in Fig. 3.1, thus the effective transmission rate is $(N - 1)/N$ the claimed rate. Note that bit power $E_b = E_s/m$ and $E_p/N_0 = 1/N_0$.

We first compare the detector performance for time-correlated channels in Figs. 5.1 and 5.2, where BPSK modulation is used to achieve a rate of 3 bits/transmission with frame size 5, 40, respectively and $\Phi_T = \Phi_R = \mathbf{I}_{N_T}$. As can be seen, the proposed detector $\hat{\mathbf{X}}_T^{\text{DDML}}(k)$ outperforms $\hat{\mathbf{X}}^{\text{MM}}(k)$ significantly in all cases, especially when the channel variation is serious. This is because in such case, the channel estimated by treating the data detected by $\hat{\mathbf{X}}^{\text{MM}}(k)$ as pilot is not reliable and may continue to affect the following data detection. In addition, what also can be seen is that a shorter frame helps receiver to get rid of this error propagation phenomenon the decision-directed method inherits at the cost of higher rate loss. The result using a higher modulation order is given in Fig. 5.3.

Next, we consider another scenario, spatial-time correlated channel. The BER performance of AML detector and Mismatched detector with DD estimator are compared in Figs. 5.4-5.5. The frame size is 5 with 3 bits/transmission for using BPSK, and the antenna spacing are 1λ , 5λ , respectively. we can see that the proposed approximated ML

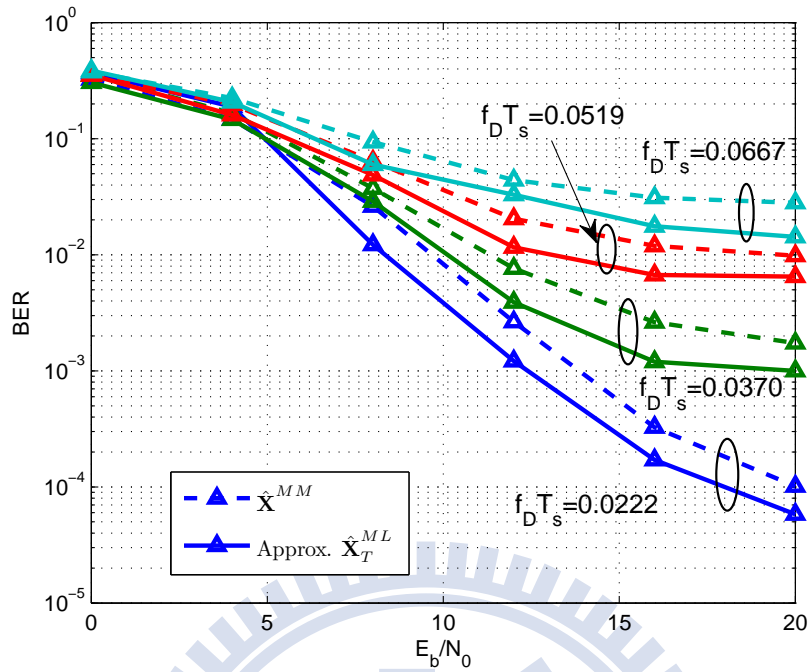


Figure 5.1: BER performance comparison of the Approx. ML and mismatched detectors using decision-directed channel estimator in time-correlated channel; 3 bits/transmission, $N = 5$.

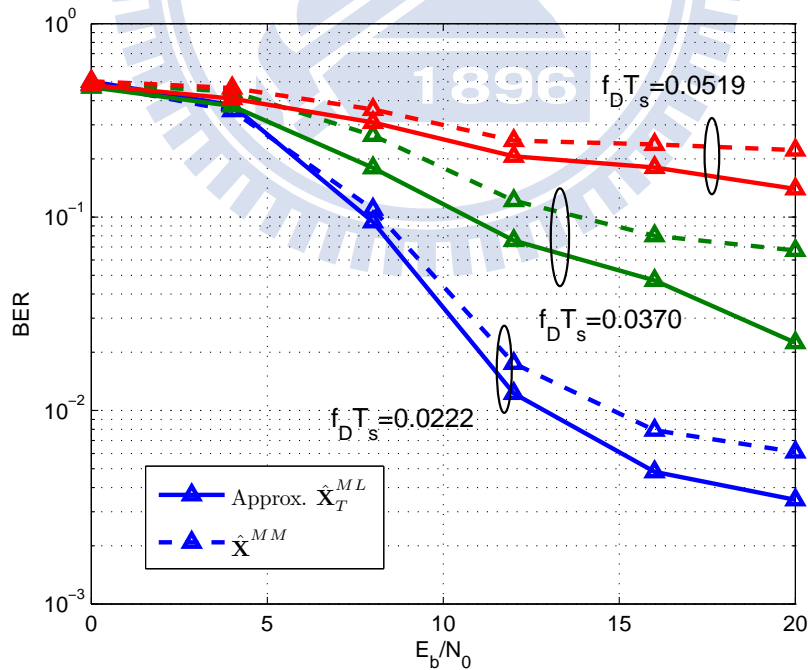


Figure 5.2: Performance of various detectors with decision-directed channel estimate in time-correlated channel; 3 bits/transmission, $N = 40$.

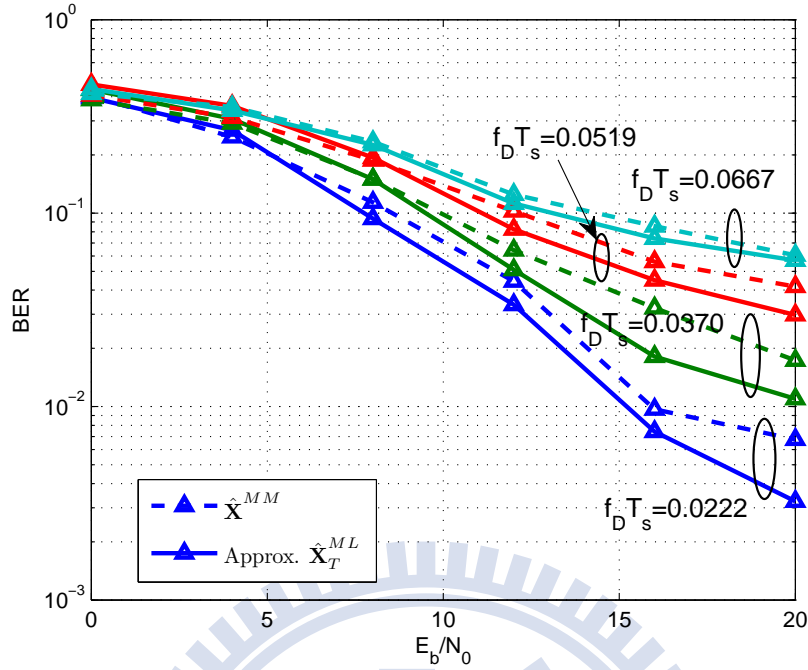


Figure 5.3: BER of Approx. ML and mismatched detectors using decision-directed channel estimate in channel with time correlation only; 6 bits/transmission, $N = 5$.

is out performance the conventional detector, although the high channel correlation will cause performance degradation to either the proposed ML detector or the conventional ML.

Next, the BER performance of AML, ML and mismatched detectors with MB and DD channel estimators are compared in Figs. 5.6-5.9 with different antenna spacing, where both spatial and time channel correlation is considered. In Figs. 5.6-5.7, the model-based estimation is applied to capture channel variation. Performance improvement is observed by using the proposed AML detector. We can see that the velocity influence more on MB channel estimator than on DD one. And the performance improvement of proposed AML detector is larger when the antenna spacing is small, i.e. high channel correlation.

Furthermore, we also show the BER performance of AML detector with MB channel estimator and estimated channel spatial correlation coefficient which is obtained in [27].

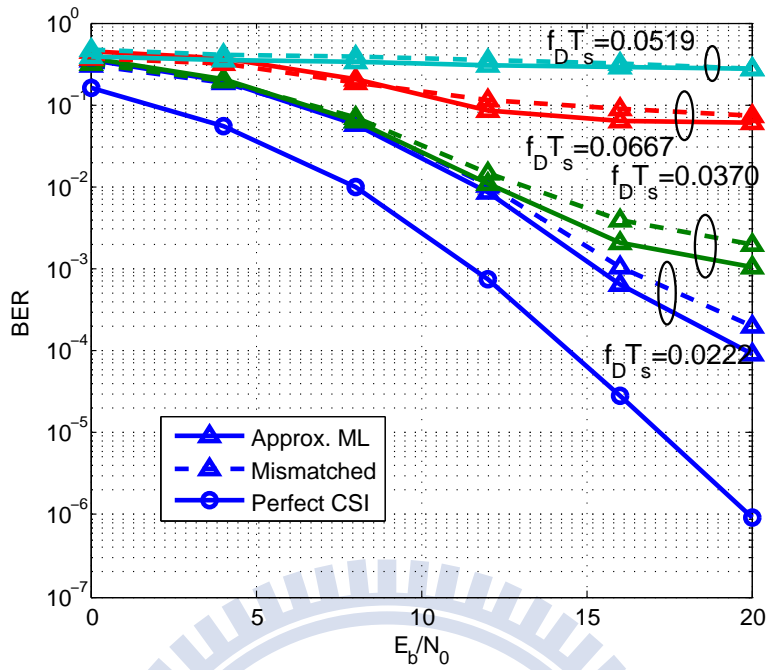


Figure 5.4: BER comparison of the Approx. ML and mismatched detectors using decision-directed channel estimator in channel with time-spatial correlation; $\xi = 1\lambda$, 3 bits/transmission, $N = 5$.

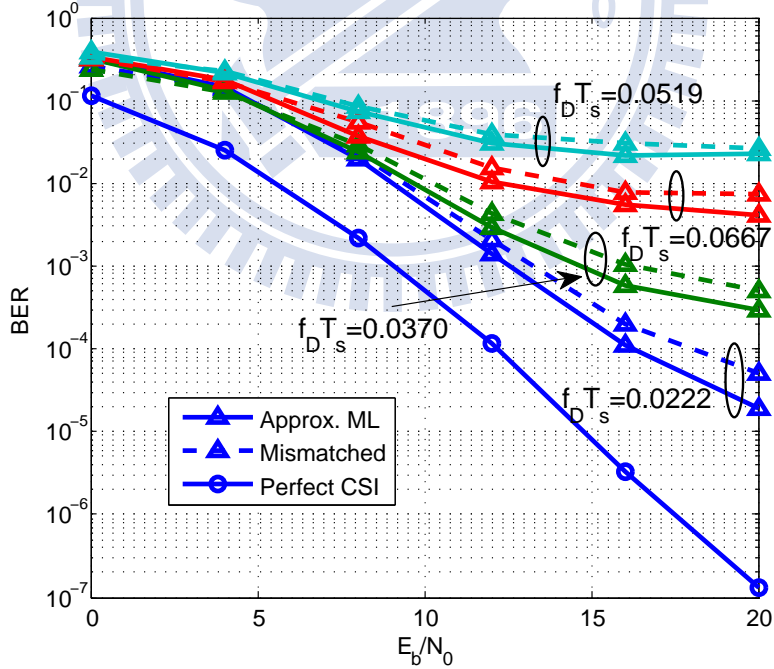


Figure 5.5: BER comparison of the Approx. ML and mismatched detectors using decision-directed channel estimator in channel with time-spatial correlation; $\xi = 5\lambda$, 3 bits/transmission, $N = 5$.

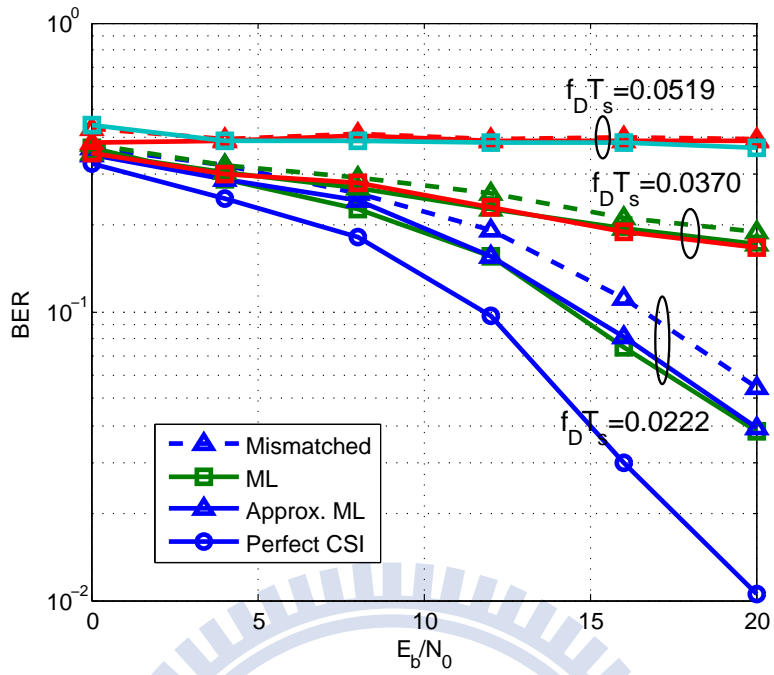


Figure 5.6: Performance of the various detectors with model-based channel estimate in time- and spatial- correlated channel; $\xi = 0.1\lambda$, 4 bits/transmission, $N = 10$ in 4×4 SM MIMO system.

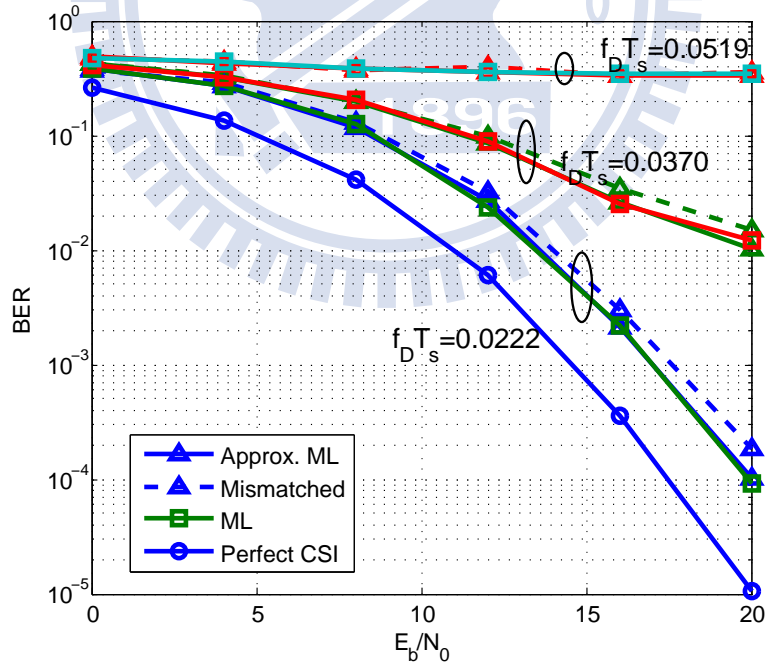


Figure 5.7: Performance of the various detectors with model-based channel estimate in time- and spatial- correlated channel; $\xi = 1\lambda$, 4 bits/transmission, $N = 10$ in 4×4 SM MIMO system.

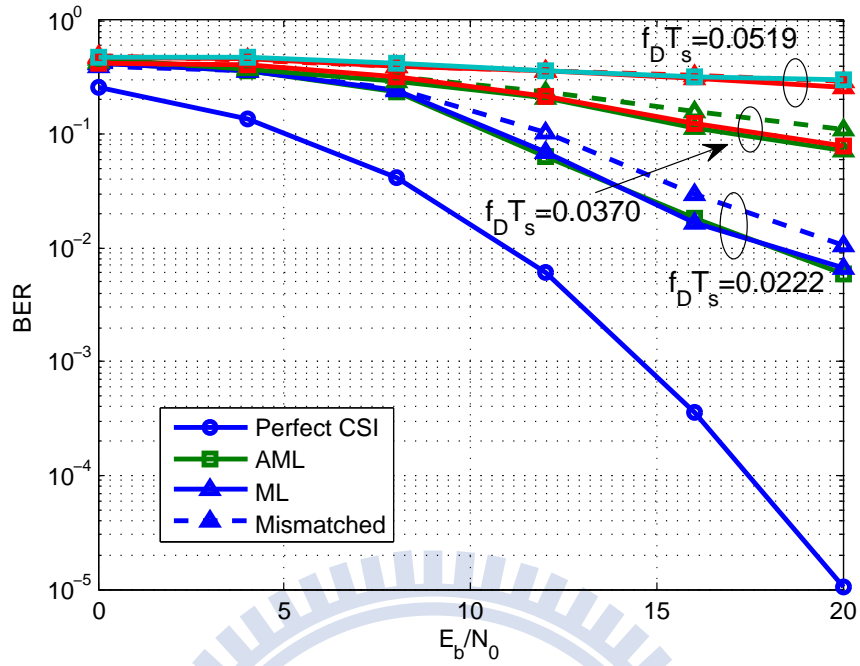


Figure 5.8: Performance of the various detectors with decision-directed channel estimate in time- and spatial- correlated channel; $\xi = 1\lambda$, 4 bits/transmission, $N = 10$ in 4×4 SM MIMO system.

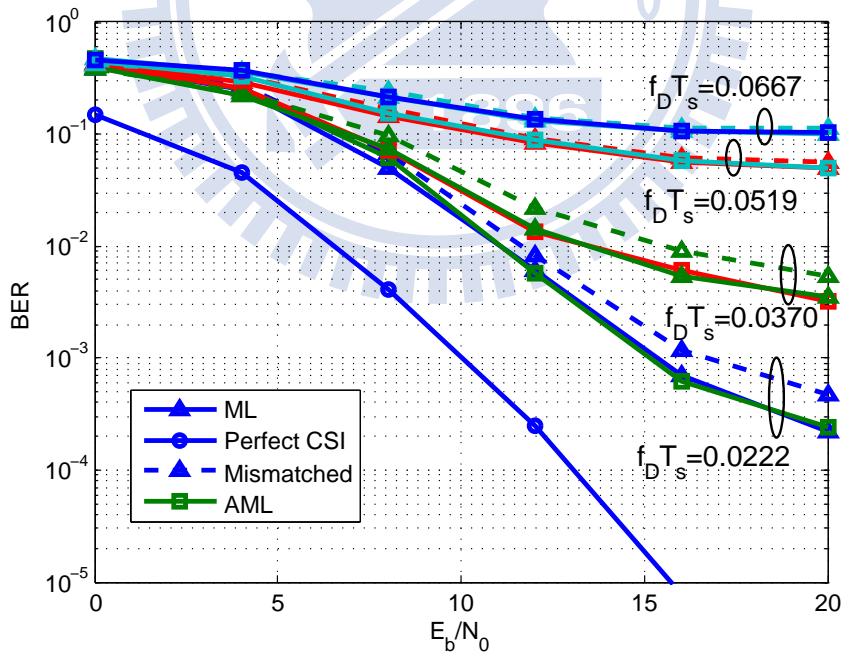


Figure 5.9: Performance of the various detectors with decision-directed channel estimate in time- and spatial- correlated channel; $\xi = 5\lambda$, 4 bits/transmission, $N = 10$ in 4×4 SM MIMO system.

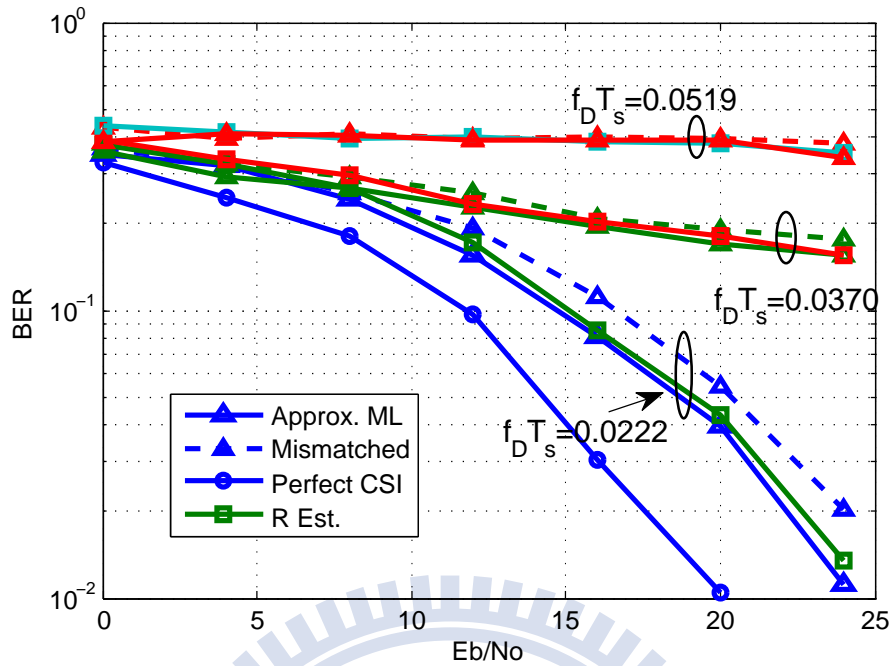


Figure 5.10: BER comparison of the approximated ML and mismatched detectors using model-based channel estimator in channel with time-spatial correlation; $\xi = 0.1\lambda$, 4 bits/transmission, $N = 10$.

The performance is a little degradation due to the estimation error of correlation coefficients, but still better than the conventional mismatched detector.

Finally, let us see the performance of the complexity-reduced AML detector. In Figs.5.13-Fig.5.15, we show the BER of complexity-reduced AML detector with MB channel estimator. We can see that the BER of complexity-reduced AML have no different from AML detector at different antenna spacing and velocity. This result is similar to 4.8 and 4.9 that the complexity-reduced method cause nearly no performance degradation to ML detector.

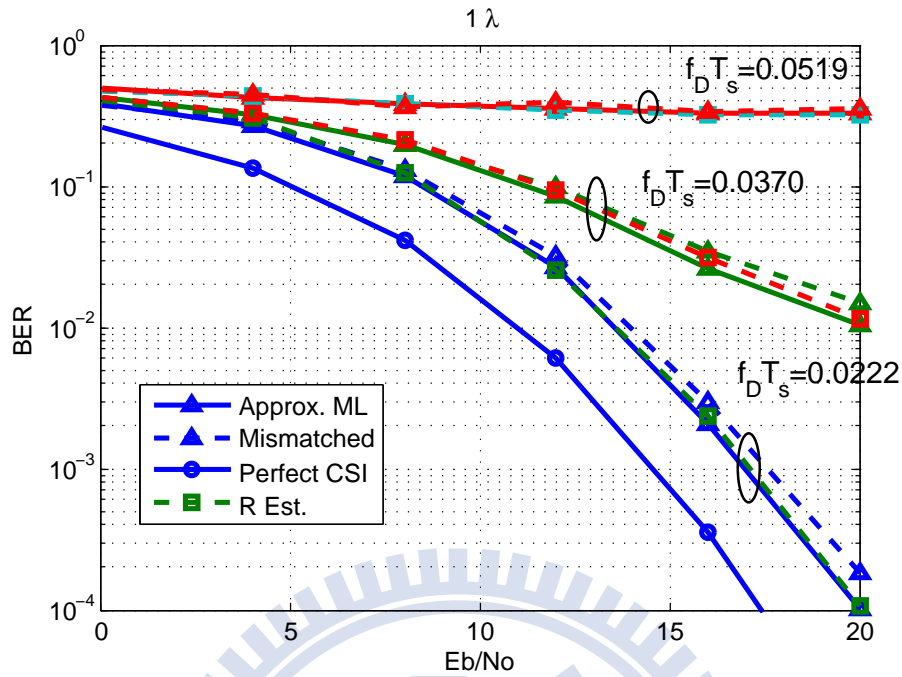


Figure 5.11: Performance of the various detectors with model-based channel estimate in time- and spatial- correlated channel; $\xi = 1\lambda$, 4 bits/transmission, $N = 10$.

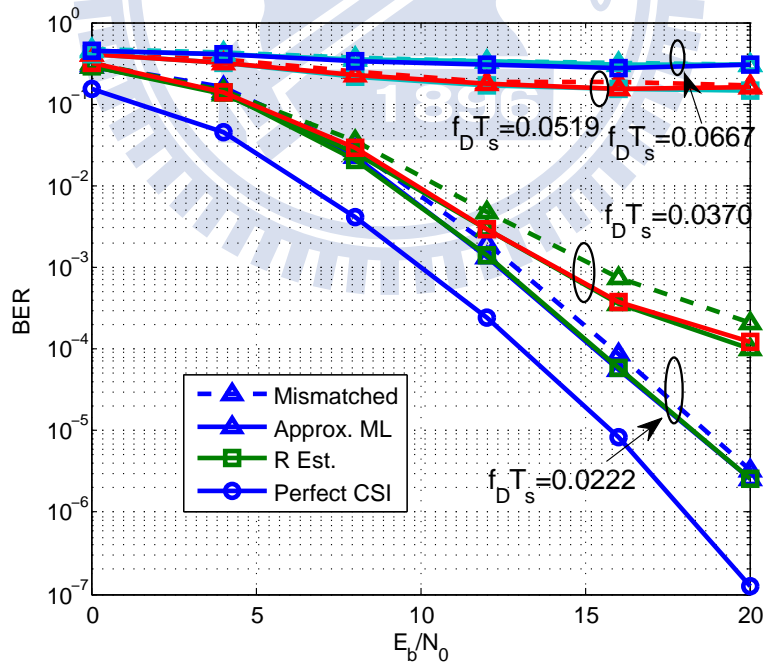


Figure 5.12: Performance of the various detectors with model-based channel estimate in time- and spatial- correlated channel; $\xi = 5\lambda$, 4 bits/transmission, $N = 10$.

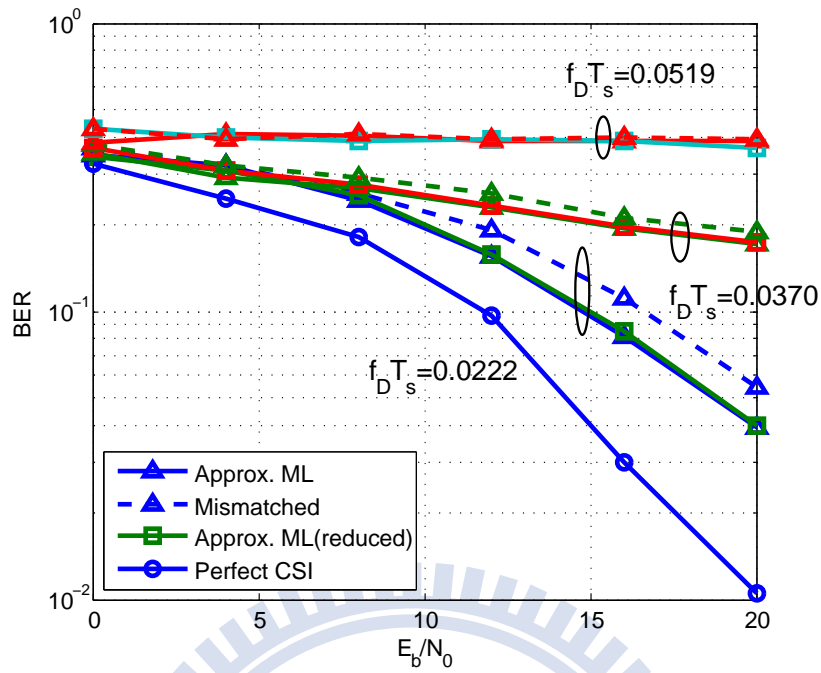


Figure 5.13: BER comparison of the approximated ML and the complexity-reduced detector using model-based channel estimator in channel with time-spatial correlation; $\xi = 0.1\lambda$, 4 bits/transmission, $N = 10$.

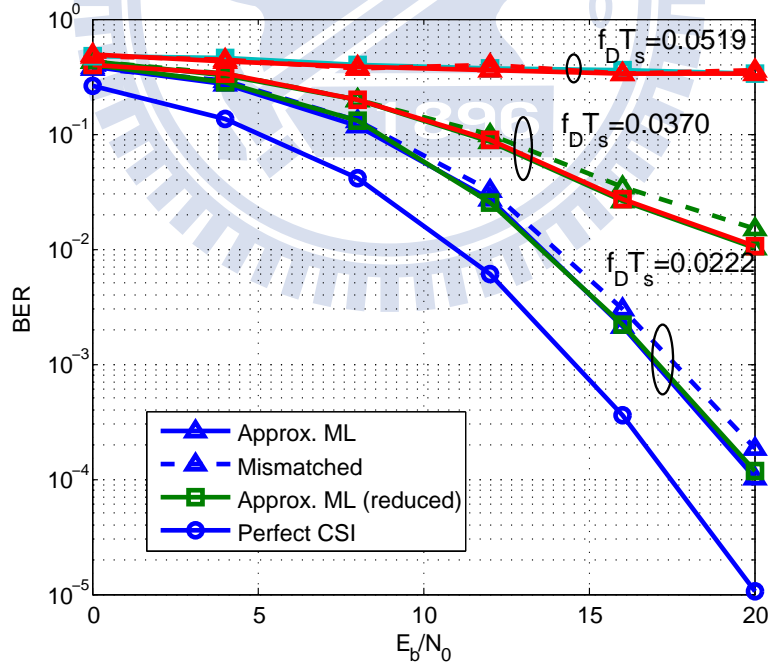


Figure 5.14: BER comparison of the approximated ML and the complexity-reduced detector with model-based channel estimate in time- and spatial- correlated channel; $\xi = 1\lambda$, 4 bits/transmission, $N = 10$.

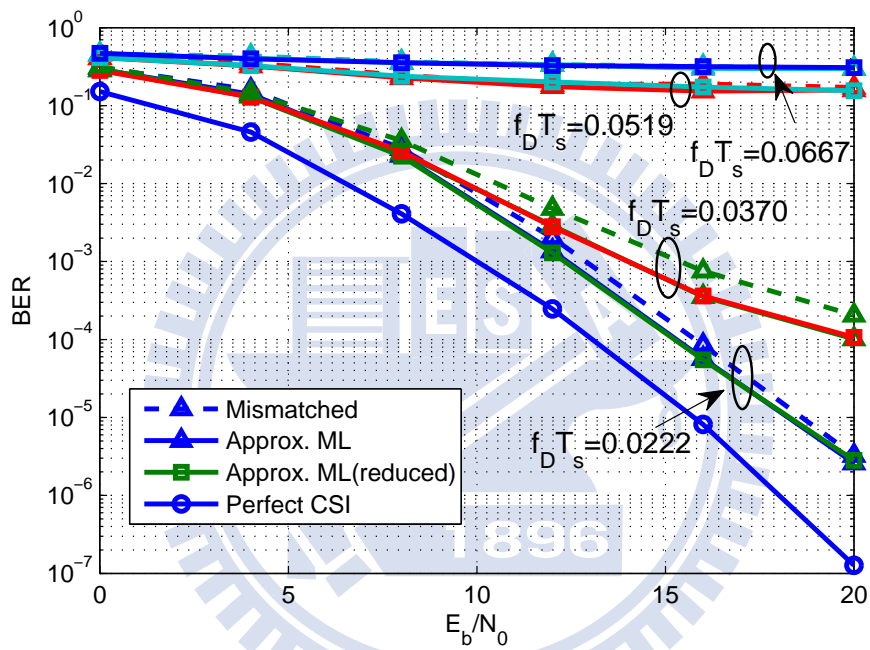


Figure 5.15: BER comparison of the approximated ML and the complexity-reduced detector with model-based channel estimate in time- and spatial- correlated channel; $\xi = 5\lambda$, 4 bits/transmission, $N = 10$.

Chapter 6

Conclusion

In this thesis we investigated some issues associated with SM MIMO systems. We first introduce the SM scheme and its optimal detector. Then, two kinds of channel estimation have been introduced. The decision-directed estimator saves the pilot signal overhead and thus retains the data rate but suffer from the error propagation problem.

We also propose two other kinds of decision-directed channel estimators that take SNR into accounts to adjust the performance of estimator, the RLS and the LMS estimator. These two detector update the channel coefficient, with a weighting factor called forgetting factor, which is the linearly combination of the 'old' channel coefficients and the 'new' channel coefficients estimated by LS method. The performance of RLS estimator and LMS estimator are similar to decision-directed estimator due to the weighting factor changing with the SNR.

To error propagation, we proposed a model-based channel estimator which uses a polynomial to catch the channel variation. Model-based channel estimator keep the pilot signal overhead ratio and prevent from the error propagation problem and update channel coefficients every time index but there is a time delay from gather the enough pilot to solve the coefficients of the polynomial. The higher the order of the polynomial is, the larger the number of the polynomial coefficients is to be estimated causing longer

delay time. But the interval of the pilot time can be adjusted to make the delay shorter.

We also analyzed the effect of imperfect CSIR over MIMO system and SM MIMO system under different receiver strategies with time- and spatial-correlated fading channel.

By taking channel estimation into consideration, we derive the ML detector for spatial-time correlated channel with model-based estimator and decision-directed estimator, and show the BER of ML detector using model-based channel estimator in conventional MIMO system and in SM MIMO system. In both systems, the proposed detectors outperform the convention mismatched detector. Furthermore, we reduced the complexity of ML detector by maximize the likelihood function separately which causing the dimension reduction in the exhausted search space, and the complexity-reduced ML detector has the similar performance to the ML detector.

We also introduce another way to lower the complexity of ML detector. We derive the approximated ML detector for time-correlated channel and spatial-time correlated channel using decision-directed estimator and derive the approximated ML detector for spatial-time correlated channel using model-based estimator. The detector for time-correlation channel case using model-based estimator which we did not derive can easily got by setting the correlation matrix $\mathbf{R} = \mathbf{I}$ in the detector. All these detectors consider the imperfect CSIR and spatial-time correlation thus outperform the conventional mismatched detector and can be seen via the simulation results. In addition, we also show the simulation results with estimated correlation matrix which is more practical and only a little degeneration to the ideal value of correlation matrix. Note that for the detectors using model-based estimator in this thesis are general form and can be used for any spatial-time correlated channel MIMO system.

ML detector is similar to the approximated ML detector via simulation results and would degenerate to the approximated ML detector when the channel is spatial-uncorrelated.

Finally, the fact that only one antenna is active at each time makes SM a promising scheme for data transmission in highly correlated channel. Nevertheless, channel de-correlation, i.e., antenna spacing increment, improves the performance of both detectors.



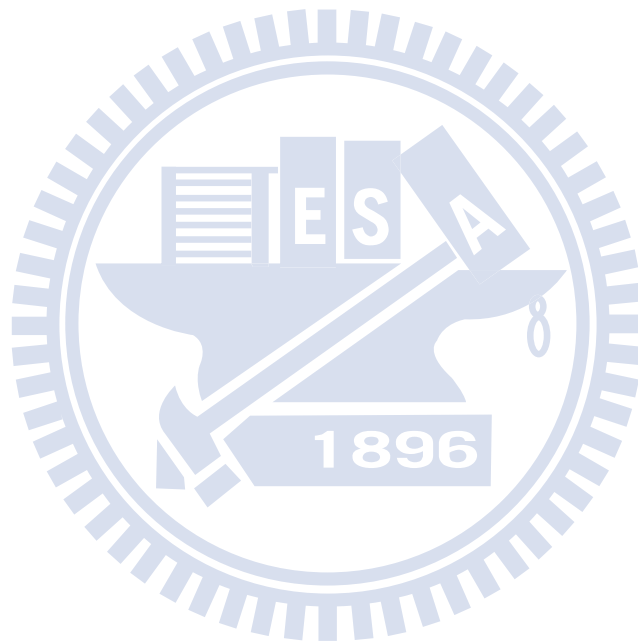
Bibliography

- [1] R. Meslsh, H. Haas, S. Sinanović, C. W. Ahn, and S. Yun, “Spatial modulation,” *IEEE Trans. Veh. Technol.*, vol. 57, no. 4, pp. 2228–2241, Jul. 2008.
- [2] F. A. Prisecaru and H. Hass. (2007) Mutual information and capacity of spatial modulation system., school of Engineering and Science Jacobs University, Germany. [Online]. Available: <http://www.eecs.iu-bremen.de/archive/bsc-2007/prisecaru.pdf>
- [3] Y. A. Chau and S.-H. Yu, “Space Modulation on Wireless Fading Channels,” in *Proc. IEEE VTC*, vol. 3, pp. 1668–1671, Atlanta, NJ, USA, Oct. 2001.
- [4] J. Jeganathan, A. Ghrayeb, and L. Szczecinski, “Space shift keying modulation for MIMO Channels,” *IEEE Commun. Mag.*, vol. 8, no. 7, pp. 3692–3703, Jul. 2009.
- [5] G. Taricco and G. Coluccia, “Optimum receiver design for correlated Rician fading MIMO channels with pilot-aided detection,” *IEEE J. Sel. Areas Commun.*, vol. 25, no. 7, pp. 1311–1321, Sep. 2007.
- [6] G. Taricco, “Optimum receiver design and performance analysis of arbitrarily correlated Rician fading MIMO channel with imperfect channel state information,” *IEEE Trans. Inf. Theory*, vol. 56, no. 3, pp. 1114–1134, Mar. 2010.
- [7] Mallik, R.K.; Garg, P., ”Optimum and suboptimum receivers for space-time coded systems in correlated fading,” *Communications, 2007. ICC '07. IEEE International Conference on* , vol., no., pp.4399,4404, 24-28 June 2007

- [8] Mallik, R.K., Garg, P., “Performance of optimum and suboptimum receivers for space-time coded systems in correlated fading,” *Communications, IEEE Transactions on*, vol.57, no.5, pp.1237,1241, May 2009
- [9] J. Zhang, Y. Zakharov, and R. N. Khal, “Optimal detection for STBC MIMO systems in spatially correlated Rayleigh fast fading channels with imperfect channel estimation,” in *Proc. IEEE ACSSC*, Pacific Grove, CA, USA, Nov. 2009.
- [10] C.-X. Wang, X. Hong, H. Wu and W. Xu, “Spatial-temporal correlation properties of the 3GPP spatial channel model and the Kronecker MIMO channel model,” *EURASIP J. Wireless Commun. and Netw.*, 2007.
- [11] C. Oestges, “Validity of the Kronecker model for MIMO correlated channels,” in *Proc. IEEE VTC*, vol. 6, pp. 2818–2822, Melbourne, Australia, May 2006.
- [12] J. P. Kermoal, L. Schumacher, K. I. Pedersen, and P. E. Mogensen, “A stochastic MIMO radio channel model with experimental validation,” *IEEE J. Sel. Areas Commun.*, vol. 20, no. 6, pp. 1211–1226, Aug. 2002.
- [13] D. Tse and P. Viswanath, *Fundamentals of Wireless Communication*, Cambridge University Press, 2005.
- [14] E. Biglieri, R. Calderbank, A. Constantinides, A. Goldsmith, A. Paulraj, and H. V. Poor, *MIMO Wireless Communications.*, Cambridge University Press, 2007.
- [15] S. M. Kay, *Fundamentals of Statistical Signal Processing: Estimation Theory*, Prentice-Hall PTR, 1998.
- [16] S. Haykin, *Adaptive Filter Theory*, Englewood Cliffs, NJ: PrenticeHall, 1996.
- [17] W. C. Jakes, *Microwave Mobile Communications*, New York: Wiley, 1974.
- [18] A. Paulraj, R. Nabar, and D. Gore, *Introduction to Space-Time Wireless Communications*, Cambridge University Press, 2003.

- [19] V. Tarokh, N. Seshadri, and A. Calderbank, "Space-time codes for high data rate wireless communication: Performance criterion and code construction," *IEEE Trans. Inf. Theory*, vol. 44, no. 2, pp. 744–765, Mar. 1998.
- [20] G. J. Foschini, "Layered space-time architecture for wireless communication in a fading environment when using multi-element antennas," *Bell Labs Tech. J.*, vol. 1, no. 2, pp. 41–59, Sep. 1996.
- [21] M. Di Renzo and H. Haas, "Performance comparison of different spatial modulation schemes in correlated fading channels," in *Proc. IEEE ICC 2010*, pp. 1–6, May 2010.
- [22] M. D. Renzo, H. Haas, and P. M. Grant, "Spatial modulation for multiple-antenna wireless system: a survey," *IEEE Commun. Mag.*, vol. 49, no. 12, pp. 182–191, Dec. 2011.
- [23] J. Jeganathan, A. Ghrayeb, and L. Szczecinski, "Spatial modulation: Optimal detection and performance analysis," *IEEE Commun. Lett.*, vol. 12, no. 8, pp. 545–547, Aug. 2008.
- [24] M. Di Renzo, R. Meslsh, and H. Haas, "Sphere decoding for spatial modulation," in *Proc. IEEE ICC 2011*, pp. 1–6, Jun. 2011.
- [25] M. Di Renzo and H. Haas, "Bit error probability of SM-MIMO over generalized fading channels," *IEEE Trans. Veh. Technol.*, vol. 61, no. 3, pp.1124–1144, Mar. 2012.
- [26] Basar, E., Aygolu, U., Panayirci, E., Poor, H.V., "Performance of spatial modulation in the presence of channel estimation errors," *Communications Letters, IEEE*, vol.16, no.2, pp.176,179, Feb. 2012

- [27] Liang-bin Li, Zong-xin Wang, “A Novel Spatial Correlation Estimation Technique for MIMO Communication System,” in *Proc. VTC, IEEE*, vol., no., pp.1-5, Sep. 2006.
- [28] G. Taricco and E. Biglieri, “Space-time decoding with imperfect channel estimation,” *IEEE Trans. Inf. Theory*, vol. 48, no. 2, pp. 359–383, Feb. 2002.
- [29] “Spatial channel model for multiple input multiple output (MIMO) simulations,” 3GPP TR 25.996 V11.0.0, Sep. 2012. [Online]. Available: <http://www.3gpp.org/ftp/Specs/html-info/25996.htm>



作者簡歷

一、About Me

- 1988 台灣台中人，出生於沙鹿。雖然是沙鹿人不過搬過很多次所以常在台中海線到處遊玩。其中沙鹿跟清水的美食小吃很棒。
- 1995 畢業於名人幼稚園。幼稚園的記憶就是一直玩遊戲吃點心，很爽快。
- 2001 畢業於鎮立沙鹿國小。國小的時候不喜歡上課都一直跟同學聊天結果被老師罵。每天休息時間就去打籃球。開始看 NBA。
- 2004 畢業於市立中港高級中學。開始感受到課業壓力，也開始喜歡上讀小說，福爾摩斯全套等偵探小說。
- 2007 畢業於國立台中一中。聞名全台灣的一中街有很多好吃的，也很好玩，有一段時間下課都跑去看漫畫。
- 2011 畢業於國立交通大學 電信工程學系。做了很多大學生所謂的瘋狂事蹟。大四的專題課程跟蘇育德老師做通訊研究專題。
- 2013 畢業於國立交通大學 電信工程研究所。因為專題研究的接續，進入蘇老師的實驗室。經過 2 年的努力地研究，終於取得碩士學位。

二、已修畢之相關課程

檢測與估計理論

數位通訊

編碼理論

隨機程序

適應性訊號處理

計算機網路

無線通訊之矩陣理論